Testing and Improving the UnTape Medical Device Concept

Carl Svanevik

A thesis

submitted in partial fulfillment of the

requirements for the degree of

Master of Science in Mechanical Engineering

University of Washington

2018

Reading Committee:

Prof. Eric Seibel, Chair

Prof. Ashley F. Emery

Mark Fauver

Program Authorized to Offer Degree:

Mechanical Engineering

University of Washington

Abstract

Testing and Improving the UnTape Medical Device Concept

Carl Svanevik

Chair of the Supervisory Committee:
Research Professor, Eric Seibel
Electrical Engineering

Strong medical tapes adhere well to the skin and different devices, however require a lot of effort to remove properly and cause medical adhesive related skin injuries (MARSIs) if done incorrectly. The goal of the UnTape project is to create a medical device, and tape that adheres strongly but is removed easily and without discomfort when desired. We will design, fabricate, and test a custom wand that will rapidly activate the photo-sensitive tape that includes active thermal feedback control of IR light, that also has 3-color LED power indicators to the user.

TABLE OF CONTENTS

LIST OF FIGURES

LIST OF TABLES

ACKNOWLEDGEMENTS

I would like to thank Dr. Eric Seibel for giving me the opportunity to join his lab and allowing me to join this project. Without him I would have never been able to learn as much as I have in the past year and a half. I would also like to thank Mark Fauver, who has mentored me over the past year and a half and taught me so much that I can't imagine where I would be on the project without him. I would also like to thank Dr. Ashley F. Emery who has made significant contributions to helping with the heat transfer portion of the project. Finally, I would like to thank my family for always supporting me and being there for me.

Chapter 1. INTROUCTION

1.1 WHAT IS A MEDICAL TAPE

A ubiquitous consumable in all hospitals, medical tapes are an integral part of supporting the care of patients. According to the FDA Code of Federal Regulations Title 21 Section 880.5240 [1], "A medical adhesive tape or adhesive bandage is a device intended for medical purposes that consists of a strip of fabric material or plastic, coated on one side with an adhesive, and may include a pad of surgical dressing without a disinfectant. The device is used to cover and protect wounds, to hold together the skin edges of a wound, to support an injured part of the body, or to secure objects to the skin." All of these duties revolve around adhesion to the skin, and often there are issues with the strength of this adhesion.

Figure 1.1. Variety of Different Medical Tapes

1.2 Medical Adhesive Related Skin Injuries (MARSI)

Strong medical tapes adhere well to the skin and to devices but are laborious to remove correctly and can cause medical adhesive related skin injuries (MARSIs) if not properly done [2]. MARSI occurs an estimated 1.5 million times annually in the United States [3] alone and incurs $4.7 - $11.6 million dollars in additional treatment costs [4]. However, tapes that are less adhesive tend not to cause skin injuries but cannot be used for life-critical systems like breathing tubes due to their tendency to lose adhesion or otherwise fail [5], [6].

There are two patient populations that are most at risk for MARSI incidence: geriatric patients and neonatal patients. In the geriatric population, several studies and reviews [7]-[13] have shown that skin tearing in geriatric patients is a clear concern due to various physiological changes in skin structure from the aging process [14]. Reductions in subcutaneous fat, cell turnover, synthesis of collagens, as well as the general remodeling and thinning of the dermis and epidermis all contribute to the decrease in skin layer adhesion and increase in susceptibility to mechanical damage. Damage such as that shown in Figure 1.2 [11] can lead to serious complications such as infection, which is only exacerbated by the slower rate of wound healing in the elderly.

Figure 1.2. Skin Stripping caused by tape removal [27]

A recent single-center observational study [13] from 2015 followed a population of older adults for 28 consecutive days and assessed the prevalence of specific MARSIs. The authors found that, on average, 13% of the patients had a MARSI on a given day; the majority of these were skin reddening and irritation. This is in line with an older 8-week study on the subject [9], claiming an incidence rate of 15.5%.

Figure 1.3. Dermatitis Caused by Irritation to Tape [27]

As compared to geriatric patients, neonatal patients are also at an increased risk MARSI, but are also more susceptible to topical agent toxicity and impaired thermoregulation as well as epidermal water loss [15]-[17]. In pediatric patients, the skin is thinner than adult skin due to fewer layers in the stratum corneum, and the epidermis is more easily separated from the dermis [18]. The incidence rate of MARSI in general is not well characterized [5], but two studies give conservative bounds of between 8% and 17% of pediatric patients [19], [20] suffering from MARSI such as skin stripping seen in Figure 1.2 [6]. In addition, unplanned extubation of breathing apparatuses is a major problem in the NICU.

The current practice for securing devices and tubes to patients is to carefully select the correct tape for the current application [2], [5], [6] based on a variety of factors including but not limited to duration of adhesion desired, criticality of adhered equipment, transparency requirements, necessity for tape breathability, and elasticity. Correct application of the tape is also important for MARSI prevention and necessitates proper training in tape usage. Solvents are

also used on occasion to help with adhesive removal, but the adhesive must be exposed and certain solvents cannot be used in pediatric patients due to toxicity concerns. This also precludes the use of many skin barrier formulations that contain these solvents.

1.3 Current Solutions

In reality, there are no current solutions that properly encapsulate the entirety of the problem that is faced, and each of the current solutions fails to meet the need of the patients and nurses in some way. Each of the solutions tackle the problem at hand differently. They have strengths and weaknesses in different areas, however no single product is able to fully satisfy the required needs. The three main popular medical tapes are kind removal silicone tapes, universal cloth adhesive tapes, paper tapes, and silk tapes. Kind silicone tape alone is a really popular product, as learned from speaking to clinicians and practitioners; they all use silicone tape regularly because of the simplicity of its use, and easy removal. Additionally, the silicone tape is non-irritating because the adhesive strength is very low, making it commonly used with simple needs. But when the time arises to securely hold a lifesaving device to a patient, silicone will not suffice due to its lack of adhesive strength.

Cloth tape and silk tape are very similar; they both use similar adhesives but have different backing, for use in varying areas and situations that may arise during practice. Cloth tape and silk tape are considered to be very strong and have adhesive qualities that are depended on to hold lifesaving devices to skin. However, while both tapes compensate for qualities which the kind remove silicone tapes lacks, they in turn have regions of weakness where the soft silicone tape is strong. Cloth tape for example, while exhibiting strong desirable adhesive strength, is also non-irritating on removal which is good, but unfortunately is quite a burden to remove. Silk tape on the other hand, is difficult to remove and also irritating to the skin. Overall,

these products are able to give partial solutions to the problem, but clinicians must weigh the benefits and weaknesses of each product before proceeding to application.

There are patents for different types of strong adhesives and weak adhesives, along with their backings, but they still fail to completely address the problem in its entirety; a new technology is required. There is another university that has been developing a medical tape and has filed for a patent, and states that it is currently working on regulation approvals that will be completed through safety tests on human adults. Researchers at the Massachusetts Institute of Technology (MIT) have been developing a medical tape that seeks a similar objective as UnTape seeks to fulfill: a tape that is strongly adhesive, comes off easily and is non-irritating. Their target population is the exact same as ours and claim that their product can also work for elderly patients. Their paper was published in *Proceedings of the National Academy of Sciences* & PubMed Central in November of 2012 [22, 26].

The premise of the design concept for MIT's "Quick-release medical tape" is that unlike normal medical tapes which have two layers, one being the adhesive and the other being a backing, their tape has a third layer. This third layer lies between the backing and adhesive and facilitates the removal of the tape. This third layer contains a laser-etched release liner which causes the tape not to be torn from the skin, nullifying any sort of stresses or strain on the skin during removal. This process of removal leaves some residual adhesive on the skin which MIT claims is easily washed or rolled off. From searching the market, it seems that this product is not readily for sale, which could either mean it is still in testing or there have been roadblocks along the testing process.

1.4 Unmet Needs

There is an abundance of unmet needs that are desired to be addressed due to that not any of the current solutions are able to completely fulfil each and every critical desired metric. The desired needs that UnTape wants to solve can be boiled down to three statements:

1) A way to address the need for reducing the incidence of MARSI so as to minimize skin tearing and irritation.
2) A way to address the need for a tape that adheres strongly to not only skin but life saving devices and comes off easily without discomfort.
3) A way to address the need for a tape that is easily removed so as to allow nurses to more effectively use their time.

1.5 Proposed Solution

Our proposed solution is to use a photosensitive and thermosensitive UnTape which changes adhesion when elevated in temperature. The goal is for UnTape to be as strong as the high strength tapes used by nurses under normal working temperatures, and then when UnTape is heated to its threshold temperature, the adhesion strength will drop off to the point where it is as weak, or weaker in adhesion than the weakest tapes used by nurses. The UnTape is made from a tape product called Intellimer, created by Nitta [33].

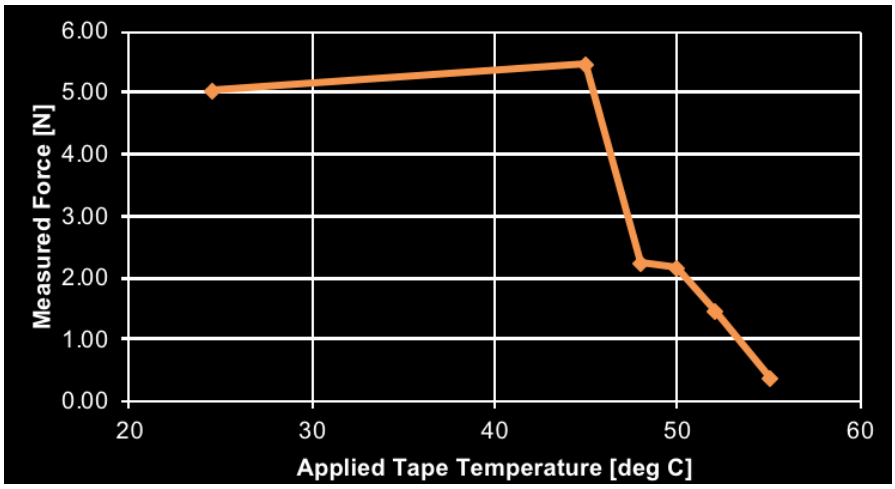

Figure 1.4. Initial Testing of UnTape Force Drop

In order to activate the tape, we will be designing an UnTape wand that outputs optical power in the near-infrared range (NIR). The primary reason for using a wand is to be able to accurately monitor and control the temperature of the tape with a feedback system. The UnTape is coated with an NIR dye that absorbs a large amount of the optical power output distributed by the wand and converts it into heat. In order to control the temperature of the tape and skin there is a thermal feedback loop that will modulate the optical power output through the use of a PID controller. This device will give nurses and administrators the ability to have a dynamic tape which can fit the needs of almost any situation and replace the requirement for an abundance of different tapes for different situations. It should be noted that the only versions of UnTape we could attain had switch temperatures at 50C° and needed to be heated to 55C° to see adhesion drop, as shown in Figure 1.4. In order for this tape to be used on skin, the switch temperature will need to be brought down substantially, such that at around 44C° we see the adhesion drop we currently see at 55C°.

Chapter 2. ADHESION DATA COLLECTION

2.1 Peel Strength Test Apparatus

Before creating prototypes and models, it was required to have a method for testing the adhesion strength of a variety of medical tapes, so that we could characterize our UnTape product, alongside with recommended medical tapes referenced by nurses. The peel strength test apparatus created is used for the physical testing of the tape itself. It is used to pull the tape from a stationary position and measure the force of adhesion. The reason for needing this comparison was to be able to create benchmarks of how our tape compares to products currently in the market. Instead of purchasing an expensive device on the market we decided to construct our own peel strength test apparatus, which is the silver instrument pictured below on the right side next to the black box in Figure 2.1.

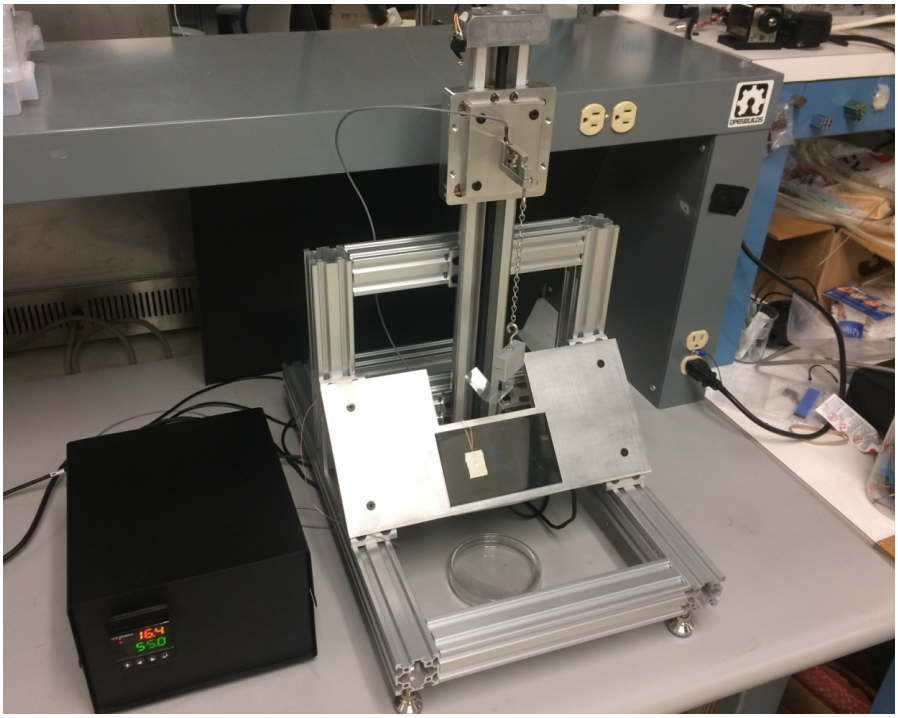

Figure 2.1. Peel Strength Test Apparatus

Most of the static structure in Figure 2.1 is made up of aluminum pieces that are attached together and connected through the use of an assortment of nuts and screws. The main components of the peel strength test apparatus are a Simo Series linear motion platform, a strain measurement device (load cell), a platform near the bottom of the structure angled at 45° to the normal, and a tape holder attached by chain to the strain measurement device.

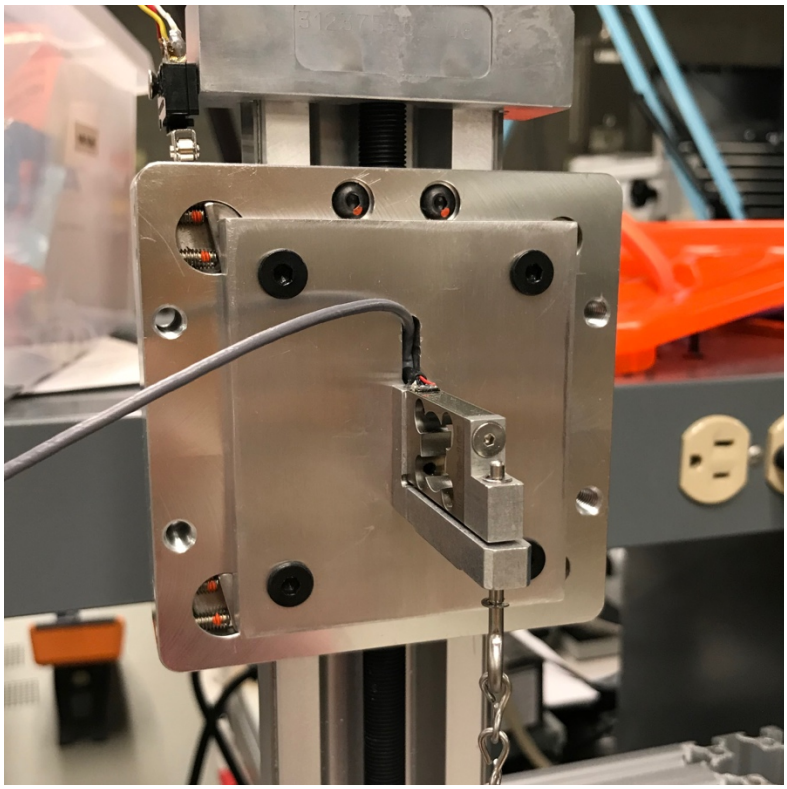

Figure 2.2. Linear Motion Platform with Customized Part and Load Cell

The linear motion platform contains a plate that moves up and down. There are limit switches at the top and bottom of the domain which act as a safety mechanism to turn off the apparatus if it moves too far up or down before causing damage to the structure. On the front surface of the platform there is a machined aluminum piece designed to allow the strain measurement device to be attached comfortably. Attached to the strain measurement device is a chain with a machined tape holder dangling at the end. The tape holder is what we use to connect different tapes to the strain measurement device so that we can test adhesion strength. The tape

holder is comprised of two different parts, one being the base and the second part being a removable cover that we use to clamp on tapes, and secure with two screws.

Figure 2.3. Tape Holder and Chain

Below the tape holder is an aluminum plate angled at 45° from the normal, with a 304-stainless-steel sheet with a brightened annealed finish used as the default substrate for testing, adhered to the center of the aluminum plate. The reason for using this substrate is because it is considered the standard material substrate used for testing and characterizing tapes according to 3M [23]. The 45° plate is adjustable in position and angle and was moved around for different tests.

The strain measurement device works by giving a linear voltage output in response to any strain it receives as input. The manufacturer's spec of the calibration constants for the strain measurement device were incorrect when tested, so we then needed to calibrate the strain measurement device ourselves. In order to calibrate the device, we used different available weights which were in the force range of the adhesion force's that we were to be measuring. The masses used for calibration were 162.6g, 298.7g, and 411.1g. The calibration curve is shown below in Figure 2.4, and was then used in the LabVIEW program.

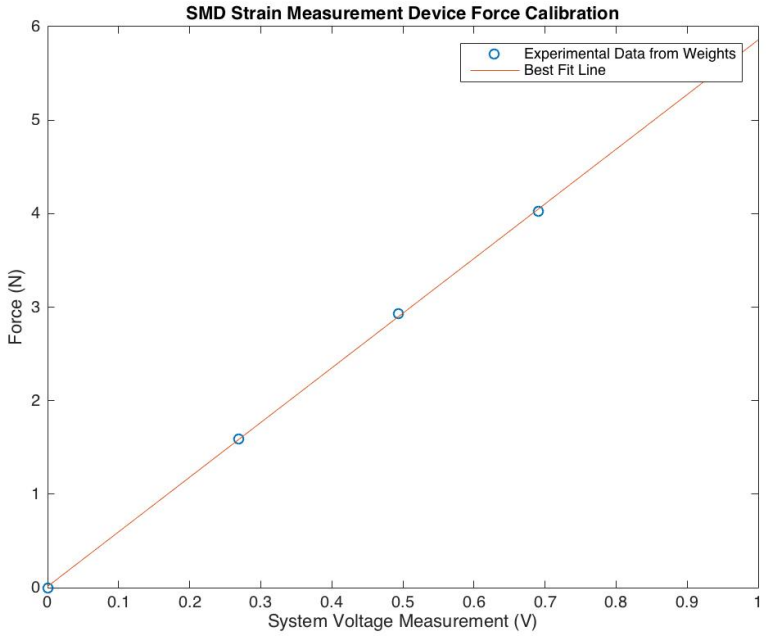

Figure 2.4. Strain Measurement Device Calibration

2.2 TEMPERATURE CONTROLLER

Next to the peel strength test apparatus in Figure 2.1 is a black box. The black box is typically referred to as a temperature controller because it is responsible for modulating the temperature of the peel strength test apparatus plate by applying energy to a heat pad located directly on the back of the angled plate. The plate will continue to heat up until the temperature read by the thermocouple located on the surface of the stainless-steel plate matches the set point programmed into the temperature controller. The temperature controller is also responsible for driving the linear motion stage up and down.

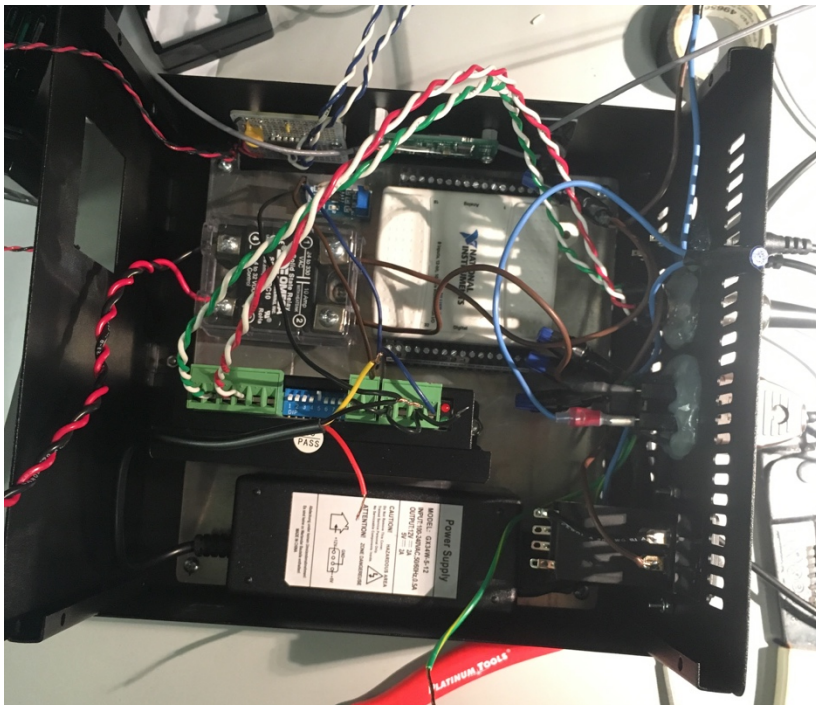

Figure 2.5. Inside the Temperature Controller

The temperature controller system is comprised of several different parts. There is a myDAQ, an impedance buffer board, a function generator, a motor driver, a stepper motor, the actual temperature controller, a solid-state relay, and a power supply all inside the outer temperature controller box. On the back of the temperature controller are inputs and outputs that go to both a laptop and to the peel strength test apparatus to control not only the linear motion platform but also the temperature of the stage. On the front of the temperature controller is an interface that lets the user view the temperature of the thermocouple and program the temperature of the plate to a desired set point. Below in Figure 2.6 is a schematic of the internal and external workings of the peel strength test apparatus and temperature controller system.

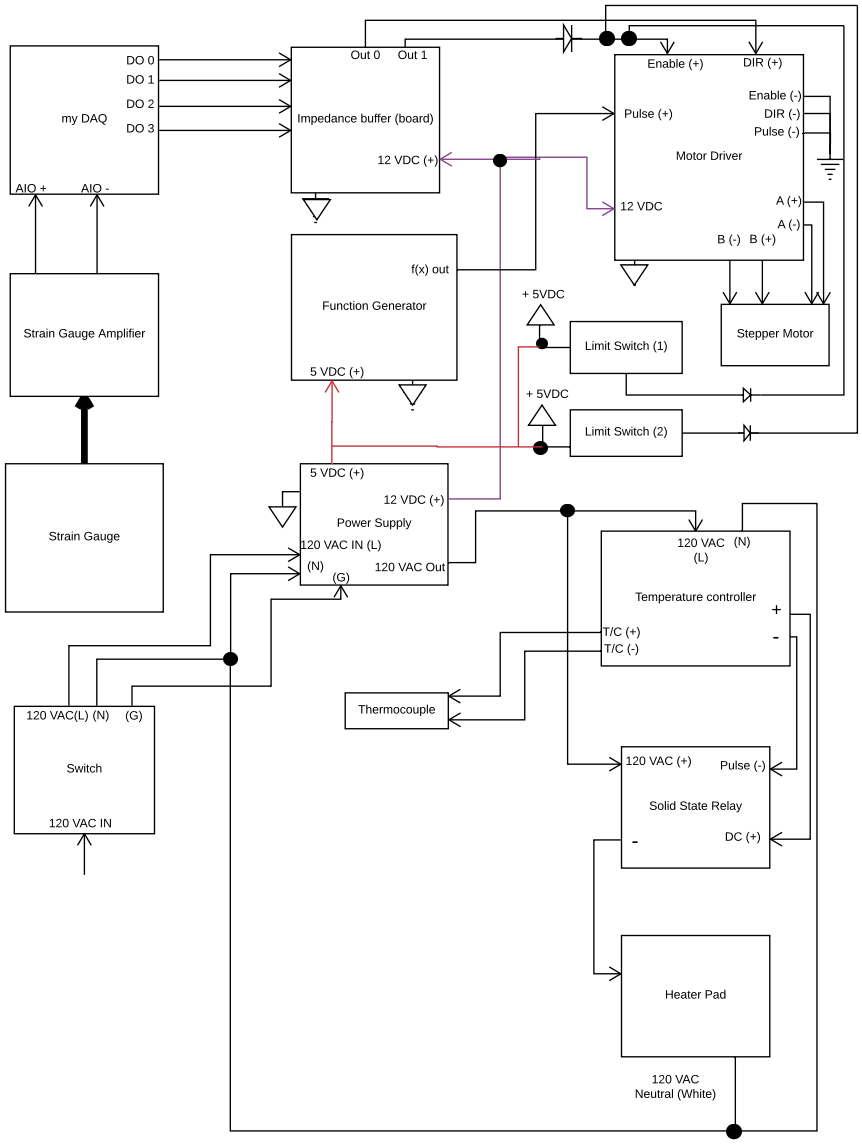

Figure 2.6. Schematic of Temperature Controller & Peel Strength Test Apparatus System

2.3 LabVIEW Program

In order to be able to gather data from the peel strength test apparatus and temperature controller, we used the myDAQ mentioned in Figure 2.5. The myDAQ box has a universal serial bus (USB) output which we connect to a laptop in order to speak to the temperature controller and peel strength apparatus. From here we created a LabVIEW program to assist in the

automation of all of our tape adhesion force testing. The user interface of the program is shown below in Figure 2.7.

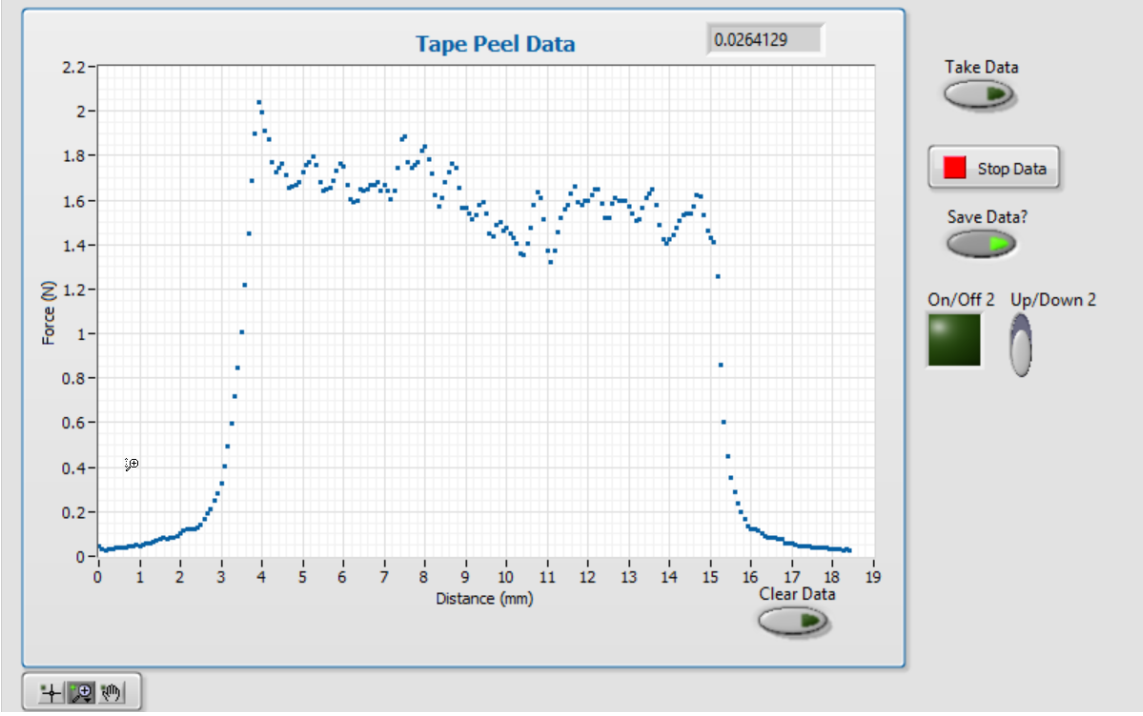

Figure 2.7. LabVIEW UI for Testing

In Figure 2.7 we can see an example of a Durapore tape test pull on the graph. In the top right corner of the graph is a dynamic readout of the current force value that the strain measurement device has measured. On the right-hand side of the graph are several buttons which are used to start a data collection trial, stop a trial, choose whether or not to save the data, and two buttons at the bottom which are used to control the location of the stage outside of testing in case we want to move or readjust the position.

Tape peel measurements last for a total of 18.3mm. The temperature controller is programmed to drive the linear motion platform at a speed of 50mm/min which means most tape pulls take approximately 22 seconds, with substrate at room temperature. Each tape pull can be separated into three sections. Initially the chain and tape holder system are not in tension with the strain measurement device, meaning that the tape is relaxed. Once the program begins, the

tension in the chain and tape holder increases with the force of the tape which in Figure 2.7 occurs from 0 to 4mm until it reaches a peak. After this first portion of the peel, the tape peel force values become more consistent as they are in constant tension, until approximately 15mm. At 15mm the linear motion platform stops translating upwards and begins moving downwards, adding slack to the chain and thus the force values decrease to approximately 0N. This allows us to take consistent measurements and lets us get more data with less tape.

A block diagram for the coding behind this program is shown below in Figure 2.8 & Figure 2.9. There are several loops at work here, however the main concept of what is going on is that data from the strain measurement device is being passed to LabVIEW and then sampled for every 100 data points, after this the data is converted from a voltage into a force value which gets displayed on the plot. While this is happening, the myDAQ is also telling the linear motion platform to rise, while measuring how far the device has travelled upwards and determining whether or not it needs to continue proceeding upwards or not.

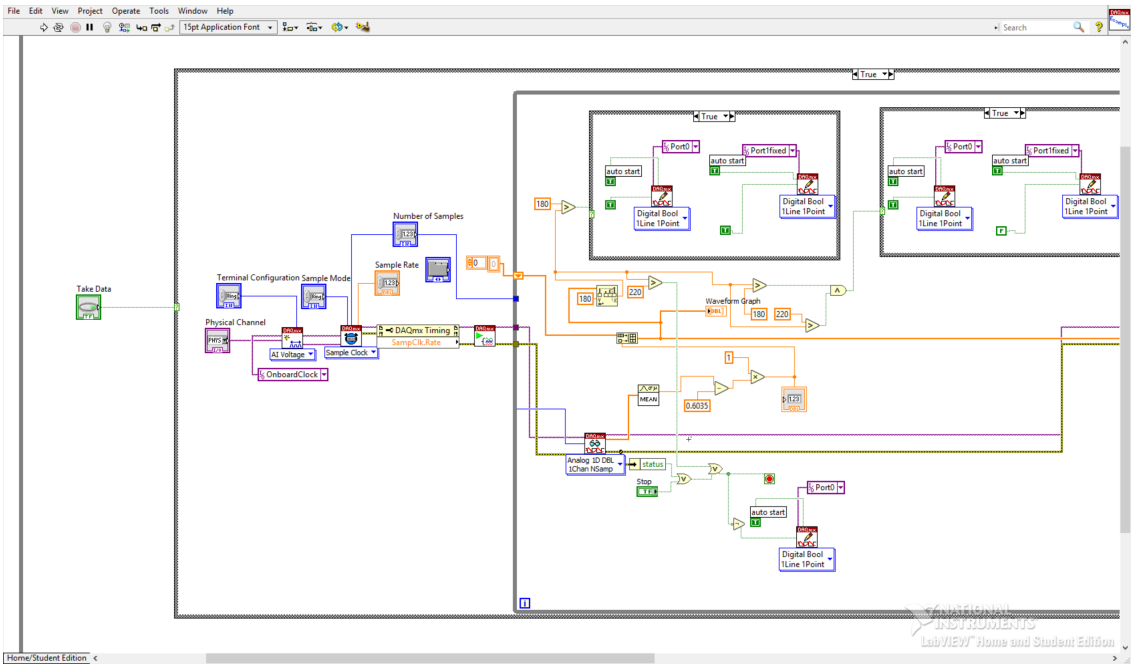

Figure 2.8. LabVIEW Block Diagram Code 1

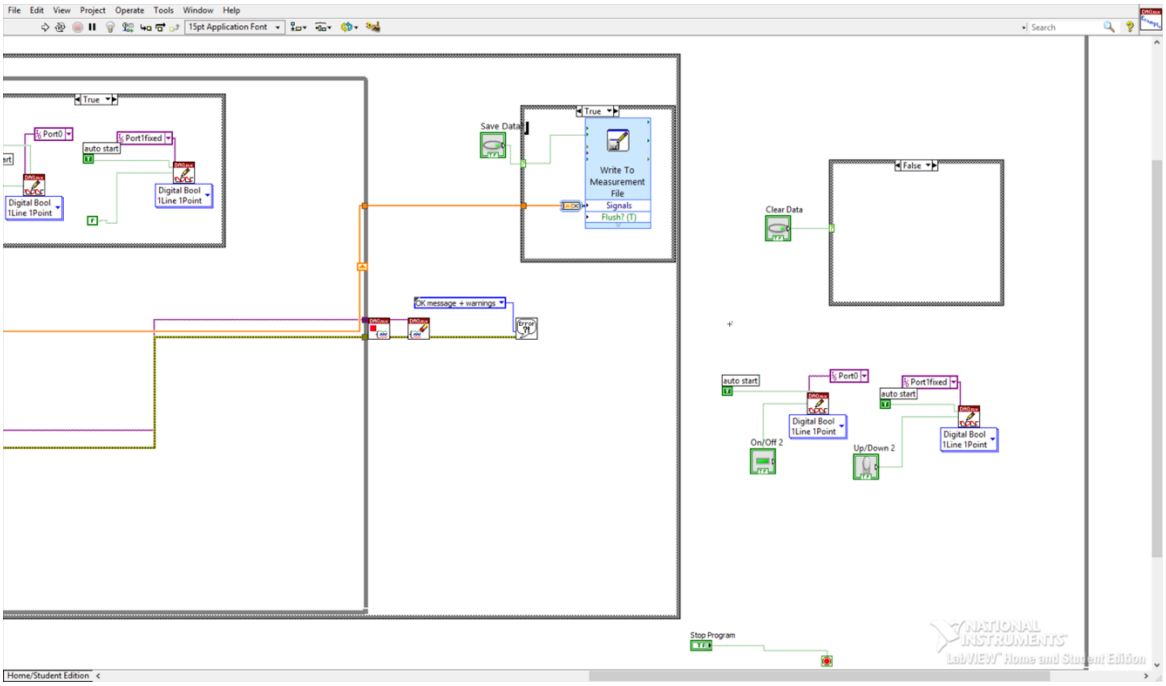

Figure 2.9. LabVIEW Block Diagram Code 2

Once the program concludes, we are able to write our data to an excel file used for later processing in Matlab or other programs. Other coding in the program deals with the functionality of the buttons and user interface on the front panel shown in Figure 2.7.

2.4 Testing Protocol

In order to have reproduceable force measurement data it was required for us to have a standard protocol for each recorded test done with the peel strength test apparatus. Listed below is the protocol required for testing Durapore and Kind tape.

1) Put on Hardy 5 mil gloves.
2) Apply Acetone & Isopropanol to testing substrate. Apply Acetone first and then IPA before finishing with the application of Acetone. Let dry and use Kimtech wipes to get rid of residue compounds alongside with other residues.
3) Lower the stage to the proper distance based on tape length.

4) Remove the tape holder from the stage and grab a piece of the prospective tape of desired length and attach it to the tape holder. Orientate the tape such that the portion of adhesion exposed to the fingers is the portion clamped down within the tape holder.
5) Line tape up with markers above the substrate and use roller to firmly attach tape to substrate. Attach the tape holder to the chain and let tape sit for 1 minute.
6) Start the LabVIEW measurement program, then repeat step 6 until the desired amount of measurements/tape length has been covered.

The protocol for the two different types of UnTape, the medium and high tack, is slightly different because of the structure of the tape. Unlike the Durapore and Kind tapes which have only a backing and an adhesive, the UnTape has a backing, and adhesive, and a protective layer on the face of the adhesive which needs to be removed before testing. Additionally, the UnTape comes in the form of sheets which need to be sliced into pieces suitable for testing. Listed below is the protocol used for testing with the two different UnTape products.

1) Put on Hardy 5 mil gloves.
2) Using a caliper and a thin marker, an UnTape sheet is marked into pieces of tape half an inch wide. Using a paper cutter, the UnTape sheet is lined up and then cut into pieces of tape for testing as shown below in Figure 2.10.

Figure 2.10. Cut UnTape Sheet

3) Apply Acetone & Isopropanol to testing substrate. Apply Acetone first and then Isopropanol before finishing with the application of Acetone. Let dry and use Kimtech wipes to get rid of residue compounds alongside with other residues.
4) Lower the stage to the proper distance based on tape length and remove the tape holder from the stage.
5) Grab a piece of UnTape and a sharp blade. Use the blade on a corner of the tape to attempt to figure out which side is the protective barrier. Once that side is determined, orientate the tape such that the side with the protective barrier is faced downwards in the middle of the tape holder.
6) Clamp the tape holder and flip it upside down. After doing so use the sharp blade to remove the protective film from the UnTape as shown below in Figure 2.11.

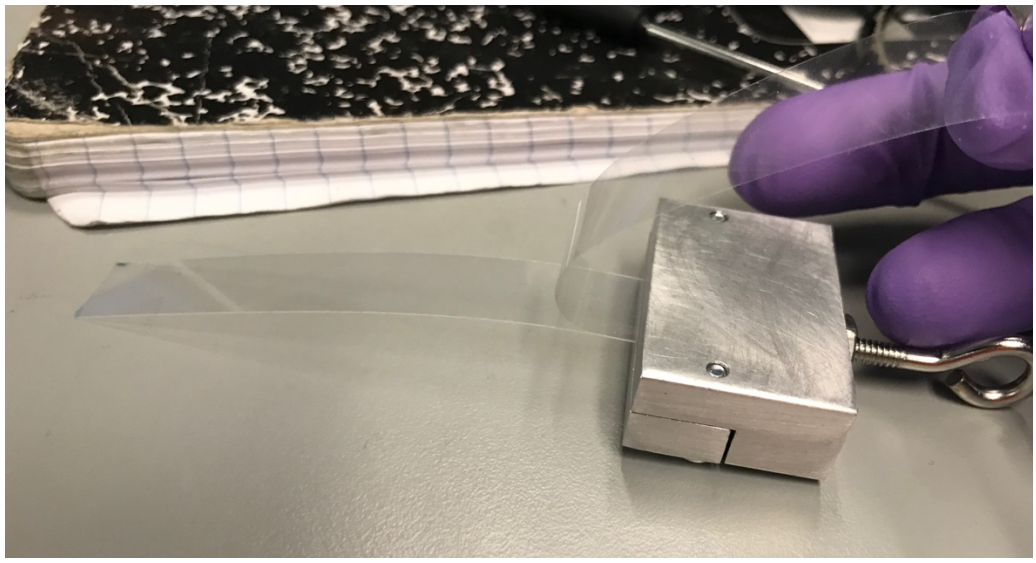

Figure 2.11. UnTape with Protective Barrier Removed

7) Line tape up with markers above the substrate and use roller to firmly attach tape to substrate. Attach the tape holder to the chain and let tape sit for 1 minute.
8) Start the LabVIEW measurement program, then repeat step 6 until the desired amount of measurements/tape length has been covered.

Chapter 3. TAPE TESTING

3.1 SUBSTRATES

The tests done in this experiment were split between two different substrates: 304-stainless-steel sheet with a bright annealed finish, and acrylic sheets. The 304-stainless-steel sheet was used as the default substrate for adhesion force testing because it is considered to be an industry standard by 3M [23] due to its reproducibility of adhesive values, making it desirable for quality control. However due to the nature of this project and being that there are thermal & heat transfer considerations to be made, we also needed a substrate that could be used to explore heat transfer of the tape in relation to skin. We couldn't use the 304-stainless-steel sheet for this because the heat transfer coefficient of steel is orders of magnitude larger than that of skin. The stainless steel would transfer heat too quickly to be able to do any sort of accurate or representable modelling of the UnTape on skin.

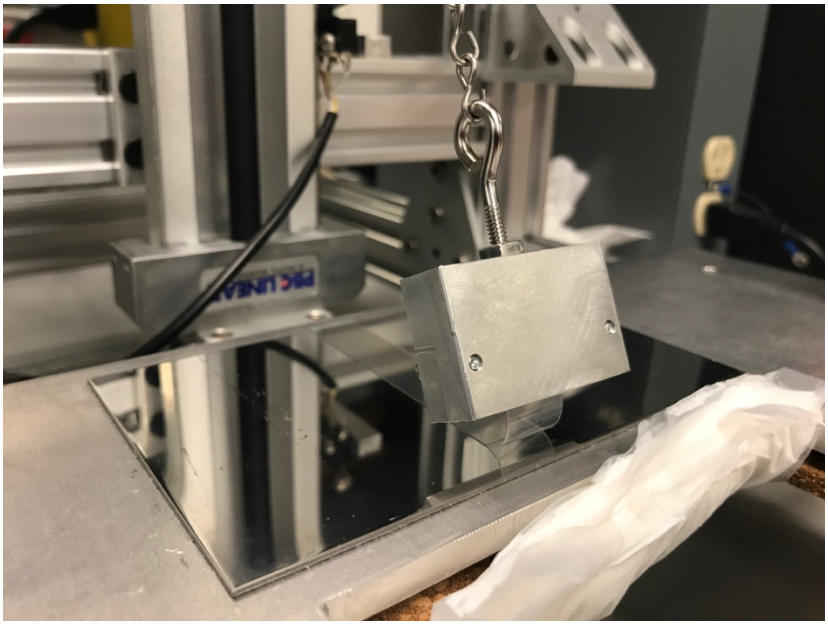

Figure 3.1. 304-Stainless-Steel Sheet Substrate

Because of this, we needed to find a material which had similar thermal properties to skin. We attempted to use different materials such as silicone or foam, however the UnTape would not adhere to them. The thermal conductivity used for skin used for all the modeling done in this research is 5 cal/cm^{2}sC° [24]. Out of all the materials, acrylic had the closest thermal conductivity (.20 W/mK [25]) of a material that was easily accessible so we used that as our second substrate for testing. Comparing the thermal diffusivity of both substrates, the thermal diffusivity of skin is approximately 5.8e-08m^2/s and that of acrylic is approximately 9.7e-08m^2/s, as calculated from [24],[25],[34],[35],[36]. Although both skin and acrylic substrates do not have the exact same thermal diffusivity, they are close enough to be able to be used to have a general idea of what will happen to the other substrate. In order to attach the acrylic substrate to the surface of the stainless-steel substrate we used double sided tape and covered the entire domain of the acrylic.

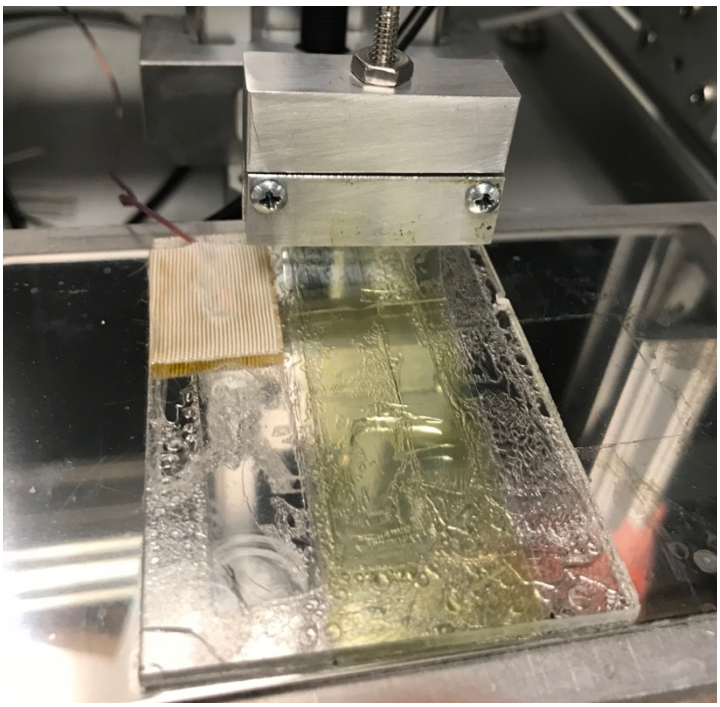

Figure 3.2. One of the Acrylic Substrates Used

The goal of testing the different tapes is that we want to show that the UnTape is as strong as, or comparable to Durapore before release, and then after release, as weak as, or comparable to the Kind tape. This way we are able to show that the UnTape is as strong as the strongest of the commonly used medical tapes, and then after release as weak as the weakest of the commonly used medical tapes by nurses. It should also be noted that due to the difference in surface properties among not only the stainless steel and acrylic, but also the skin, it is difficult to translate the measurements gathered to exact values on skin. However, if we can demonstrate the UnTape does decrease adhesion dramatically on both substrates, then there is a good change that the same will occur on skin.

3.2 KIND TAPE

As mentioned previously, Kind silicone tape was one of the tapes chosen to test due to that it is considered to be one of the weaker medical tapes used by nurses. We tested the Kind tape on both stainless steel and acrylic substrates at 90° with proper protocol. On stainless-steel, 11 trials were done where an average steady state peel force was measured to be .042N/mm with a standard deviation of .009N/mm. On acrylic, 12 trials were done with an average steady state peel force measured to be .030N/mm with a standard deviation of .010N/mm. The average peel force profile of kind tape on stainless steel substrate is shown below in Figure 3.3, and then acrylic below that in Figure 3.4.

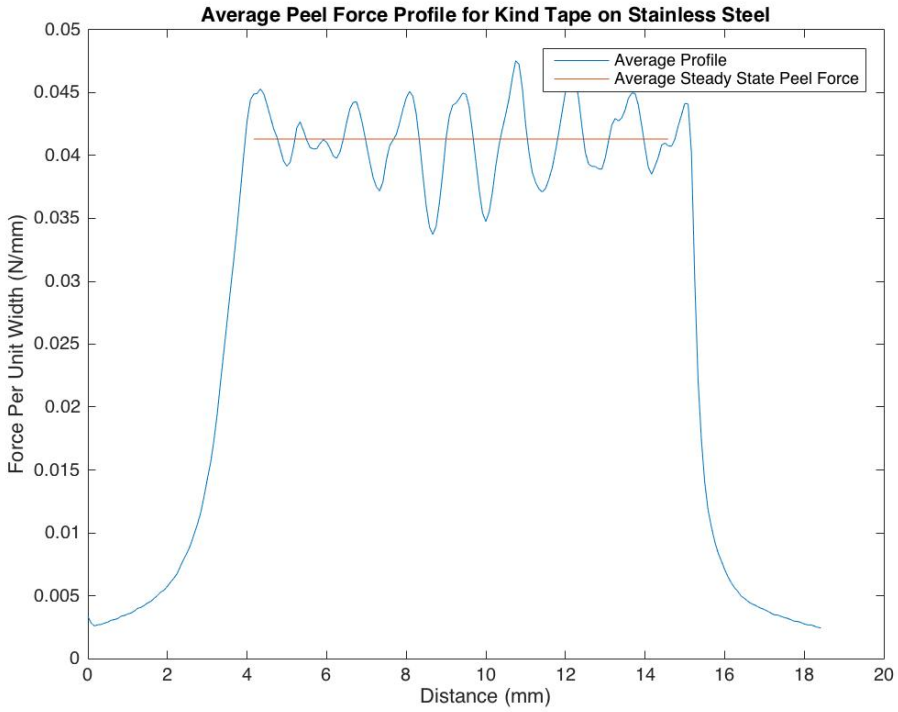

Figure 3.3. Average Peel Force Profile for Kind Tape on Stainless Steel

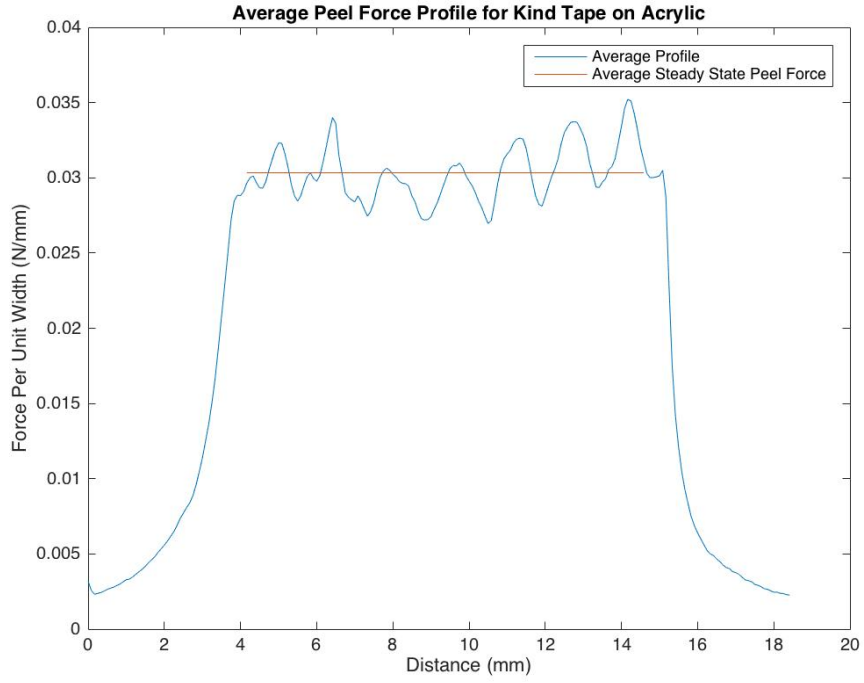

Figure 3.4. Average Peel Force Profile for Kind Tape on Acrylic

An interesting observation about the Kind tape is that when looking at the adhesion peel force profile shown in Figure 3.3 & Figure 3.4, there seems to be a sinusoidal trend or consistent increasing and decreasing trend as the peel occurs. Some of this data can perhaps be explained by looking at an image of the Kind tape backing. Although perhaps difficult to notice, as we move along the domain from left to right there are small lines going across from top to bottom of "+" and "-" symbols inscribed into the tape. It could be that these bumps in the tape are generating changes in adhesion, which would describe the continuous increasing and decreasing found throughout the data sets.

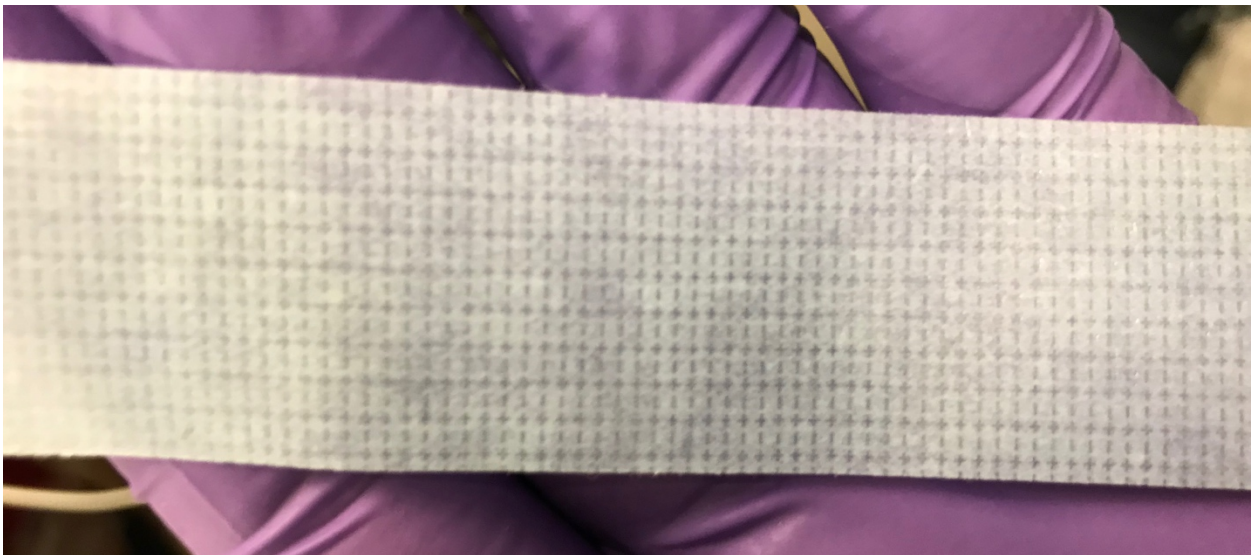

Figure 3.5. Kind Tape Up Close

3.3 DURAPORE TAPE

As mentioned previously, Durapore was one of the tapes tested because it is considered to be one of the highest tack tapes commonly used by nurses. We tested the Durapore tape on both stainless steel and acrylic substrates at 90° with proper protocol. On stainless-steel, 12 trials were done where an average steady state peel force was measured to be .100N/mm with a standard deviation of .014N/mm. On acrylic, 11 trials were done with an average steady state

peel force measured to be .206N/mm with a standard deviation of .019N/mm. The average peel force profile of the Durapore tape on stainless steel substrate is shown below in Figure 3.6, and then acrylic below that in Figure 3.7.

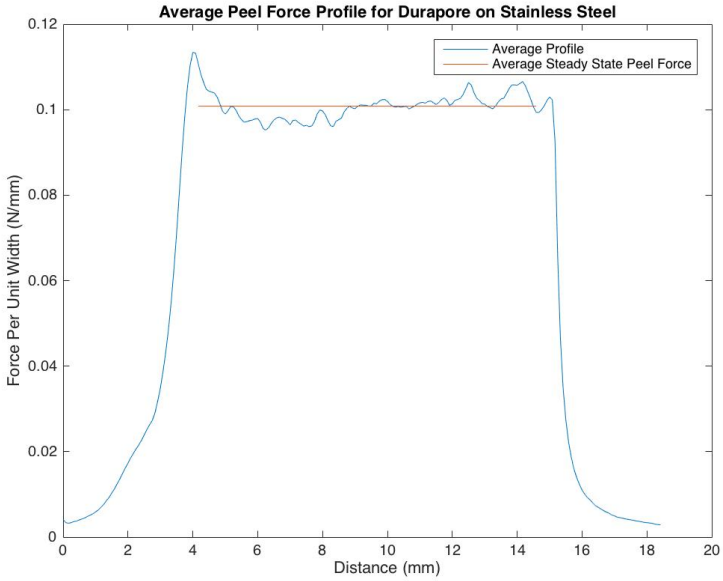

Figure 3.6. Average Peel Force Profile for Durapore Tape on Stainless Steel

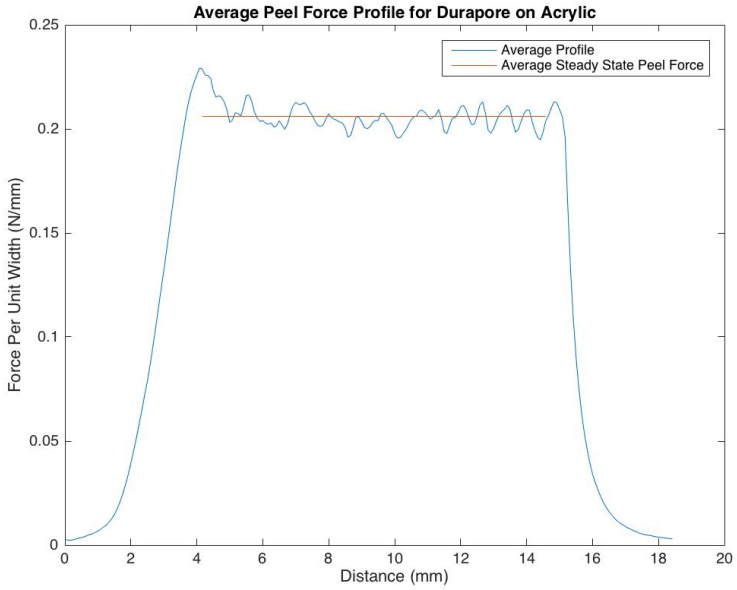

Figure 3.7. Average Peel Force Profile for Durapore Tape on Acrylic

Similar to the Kind tape, the Durapore tape has a similar increasing and decreasing adhesion effect as the tape peel tests were done. Upon examining the backing of the Durapore tape, similar conclusions can be drawn as to the Kind tape due to the similar nature in columns present on the backing of the tape as shown below in Figure 3.8.

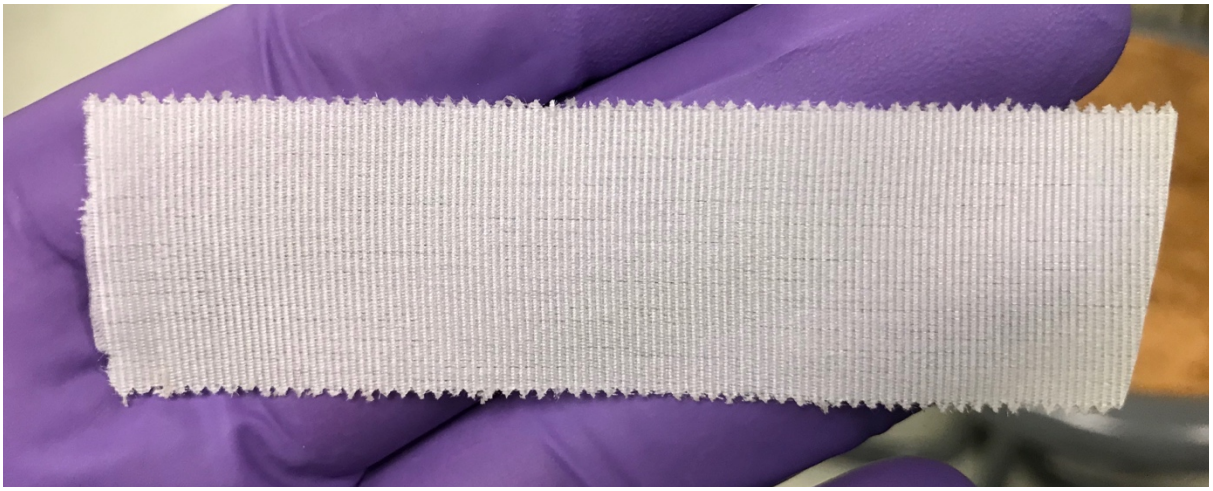

Figure 3.8. Durapore Tape Up Close

3.4 UnTape High Tack

The UnTape high tack tape was tested on both stainless steel and acrylic substrates at 90° with proper protocol. We tested a control data set on both substrates at room temperature and then tested the released UnTape at 55C° by raising the temperature of the substrate used. On the stainless-steel substrate for the control data set, 12 trials were done with an average steady state peel force measured to be .145N/mm with a standard deviation of .037N/mm. Once heated to 55C°, 6 trials were done with an average steady state peel force on stainless steel measured to be 0N/mm, as the tape was falling off before it could be peeled. On acrylic for the control data set, 10 trials were done with an average steady state peel force measured to be .382N/mm with a

standard deviation of .043N/mm. Once heated to 55C°, 17 trials were done with an average steady state peel force on acrylic measured to be the .133N/mm with a standard deviation of .034N/mm. This results in a 100% adhesion force drop on stainless steel, and a 65% adhesion force drop on an acrylic substrate. The average peel force profile of the UnTape high tack tape on stainless steel substrate before and after release is shown in Figure 3.9 & Figure 3.10, then on acrylic before and after release in Figure 3.11 & Figure 3.12.

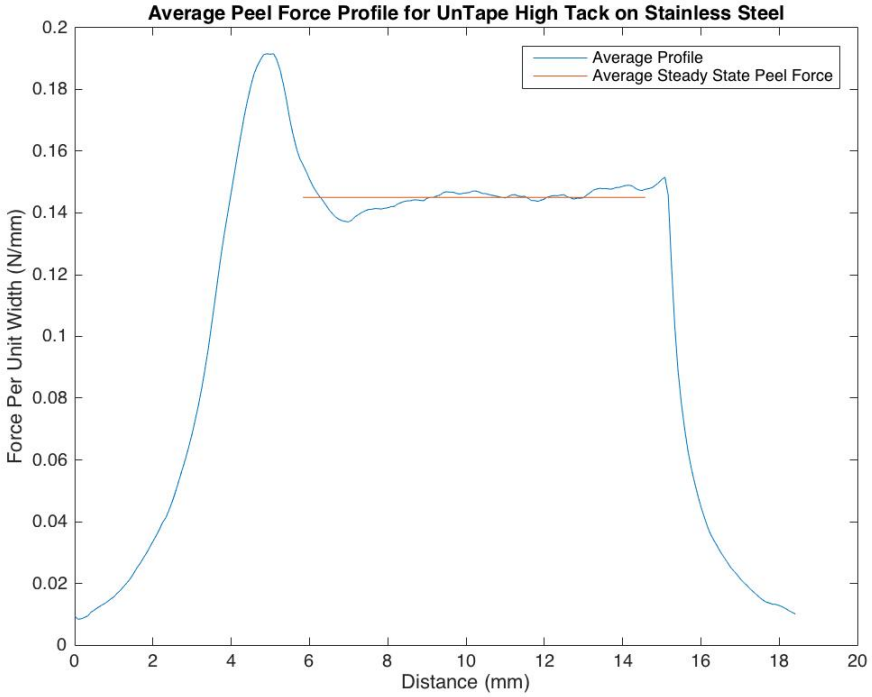

Figure 3.9. UnTape High Tack on Stainless Steel Substrate Before Release

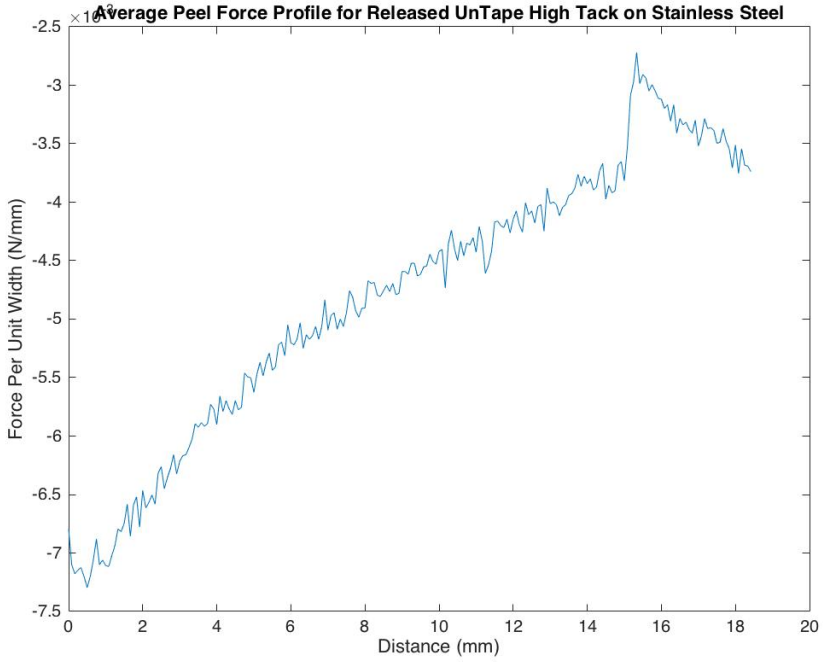

Figure 3.10. UnTape High Tack on Stainless Steel Substrate After Release

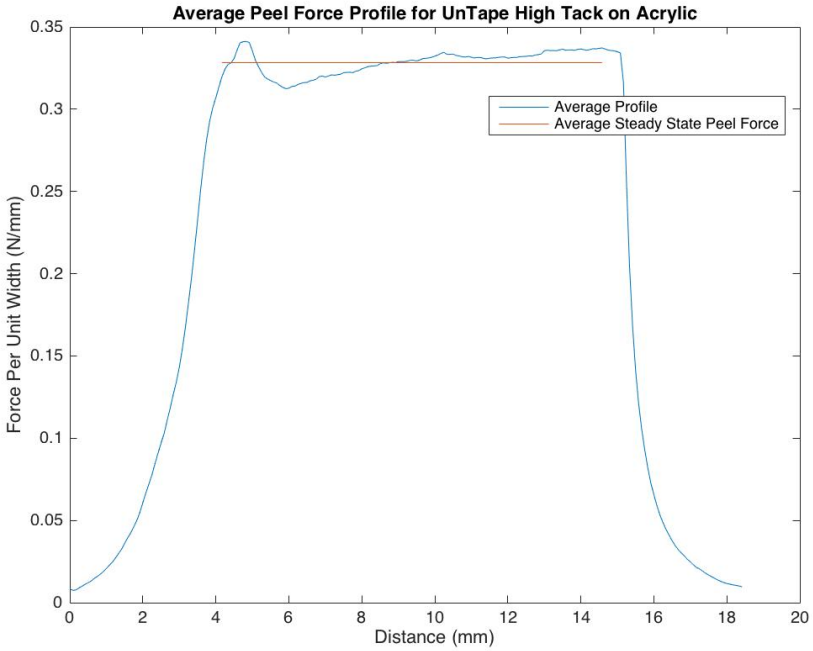

Figure 3.11. UnTape High Tack on Acrylic Substrate Before Release

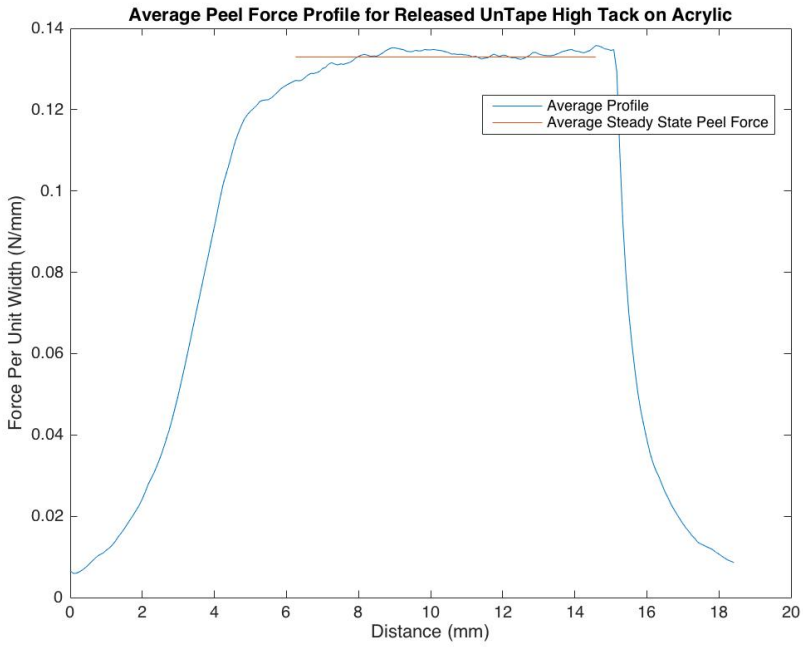

Figure 3.12. UnTape High Tack on Acrylic Substrate After Release

Due to the difference in adhesion values comparing the before and after release data of the UnTape high tack on acrylic substrate, it was hypothesized that for in order to receive a similar force drop in comparison to stainless steel, perhaps there is longer transient response on the acrylic substrate. We tested this by using the normal UnTape protocol however instead of letting the tape sit for a minute and doing continuous measurements, we took measurements in increments of approximately 1 minute in order to see if there was an extended transient adhesion force drop, however it turns out that the force values stay rather consistent after 5 minutes. This suggests that differences in adhesion drops between substrates is most likely due to the difference in substrates properties.

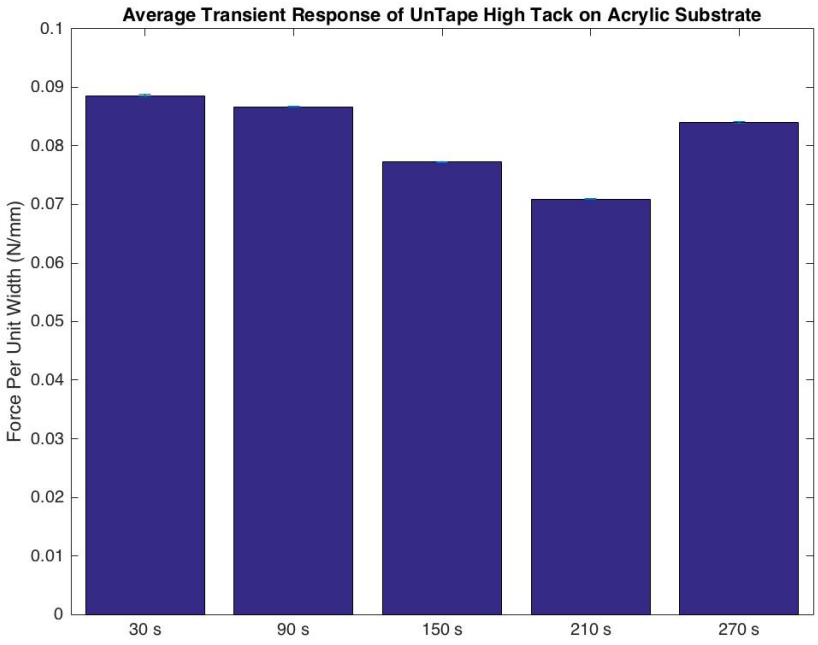

Figure 3.13. Transient UnTape High Tack Measurements on Acrylic Substrate

3.5 UnTape Medium Tack

The UnTape medium tack tape was tested on both stainless steel and acrylic substrates at 90° with proper protocol. We tested a control data set on both substrates at room temperature and then tested the released UnTape at 55C° by raising the temperature of the substrate used. On stainless-steel for the control data set, 11 trials were done with an average steady state peel force measured to be .082N/mm with a standard deviation of .014N/mm. Once heated to 55C°, 6 trials were done with an average steady state peel force on stainless steel measured to be 0N/mm, as the tape was falling off before it could be peeled. On acrylic for the control data set, 12 trials were done with an average steady state peel force measured to be .181N/mm with a standard deviation of .035N/mm. Once heated to 55C°, 18 trials were done with an average steady state peel force on acrylic measured to be the .035 N/mm with a standard deviation of .013N/mm.

This results in a 100% adhesion force drop on stainless steel, and an 81% adhesion force drop on an acrylic substrate. The average peel force profile of the UnTape medium tack tape on stainless steel substrate before and after release is shown in Figure 3.14 & Figure 3.15 then on acrylic before and after release in Figure 3.16 & Figure 3.17.

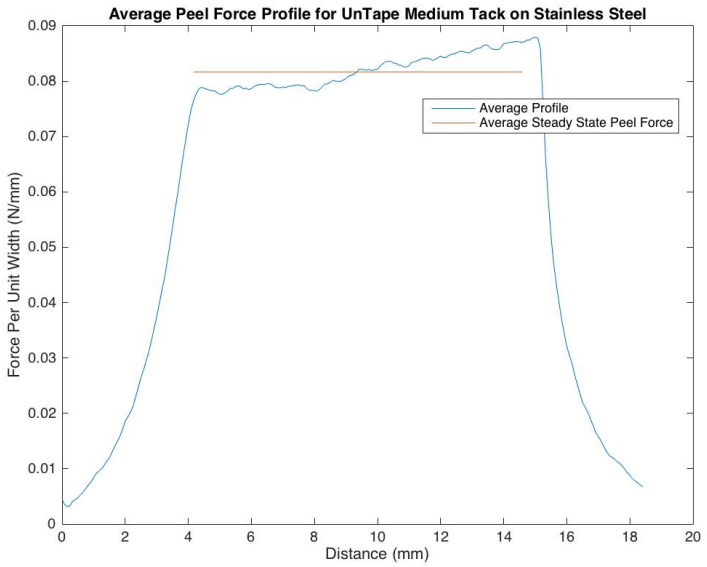

Figure 3.14. UnTape Medium Tack on Stainless Steel Substrate Before Release

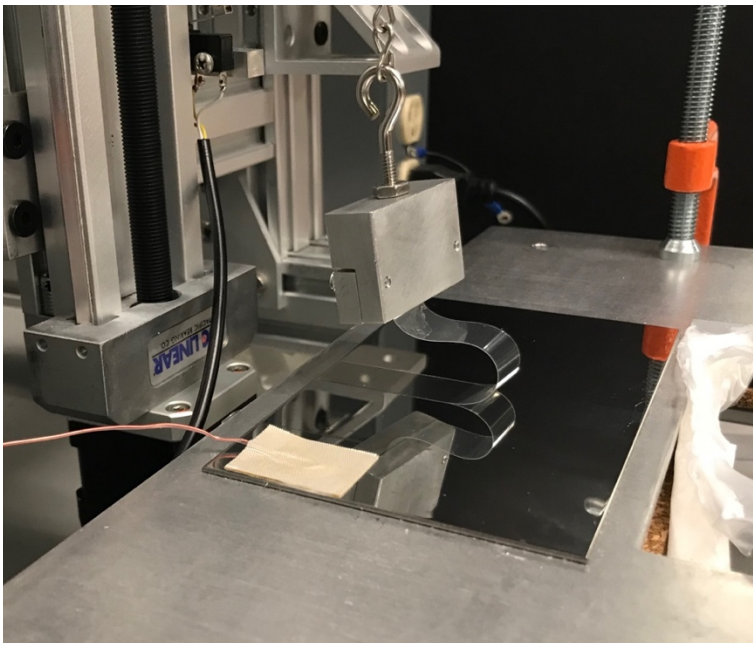

Figure 3.15. UnTape Medium Tack on Stainless Steel After Release Peeling Itself

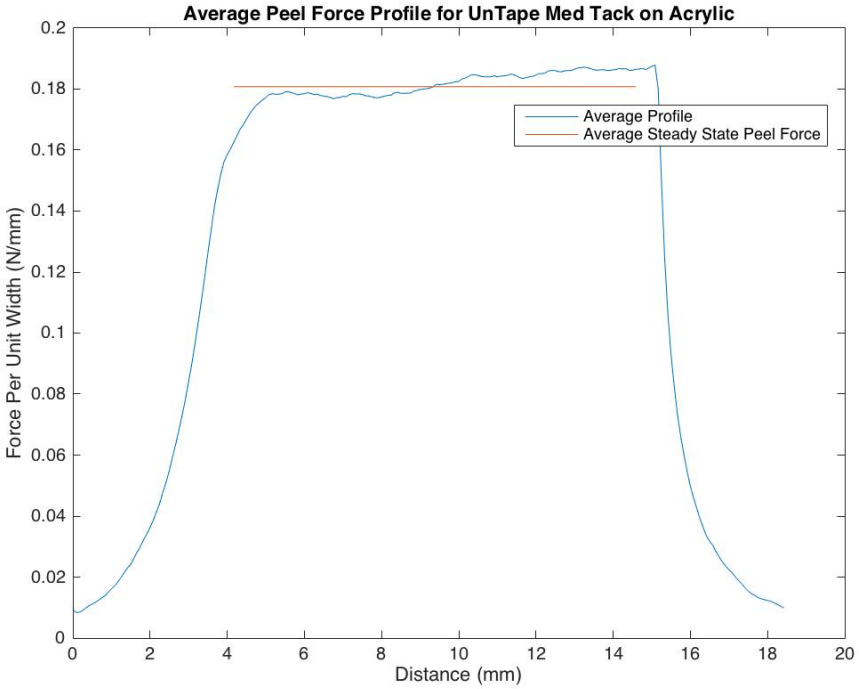

Figure 3.16. UnTape Medium Tack on Acrylic Substrate Before Release

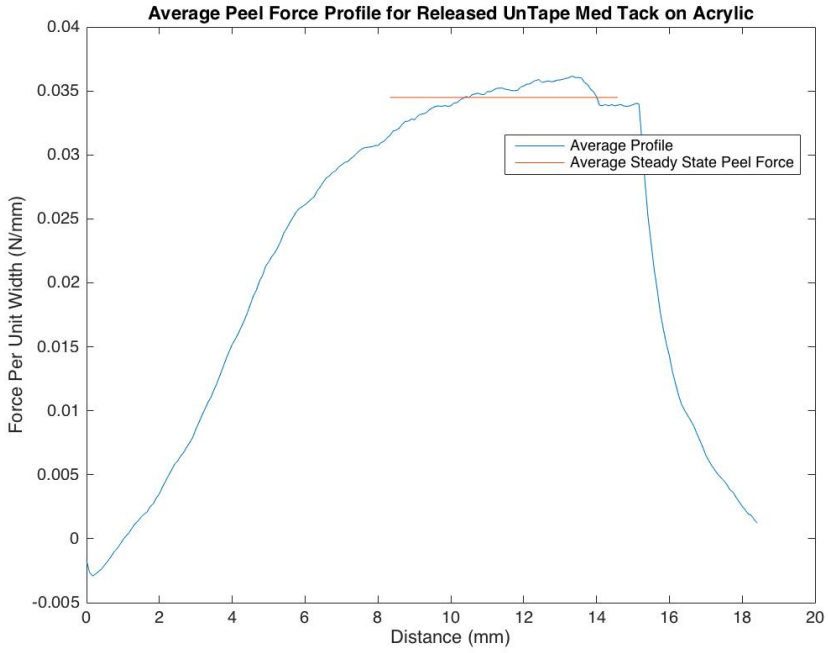

Figure 3.17. UnTape Medium Tack on Acrylic Substrate After Release

3.6 TAPE COMPARISONS

Extracting the data from the Durapore tape, Kind tape, UnTape high tack, and UnTape medium tack tape pulls and organizing them based on substrates, we receive Figure 3.18 and Figure 3.19 below, which show comparisons of the various medical tapes tested among different substrates in terms of adhesion force. The error bars denote the standard deviation for each individual data set as listed in each tape's respected sections.

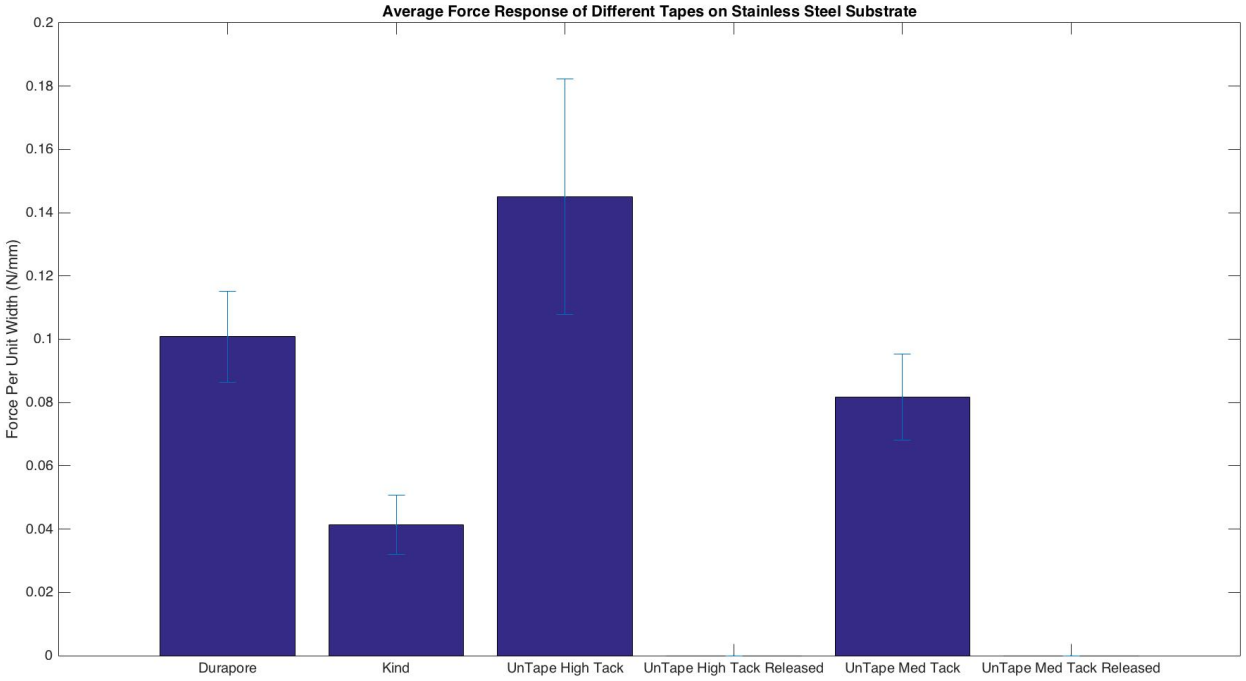

Figure 3.18. Medical Tape Comparisons on Stainless Steel Substrate

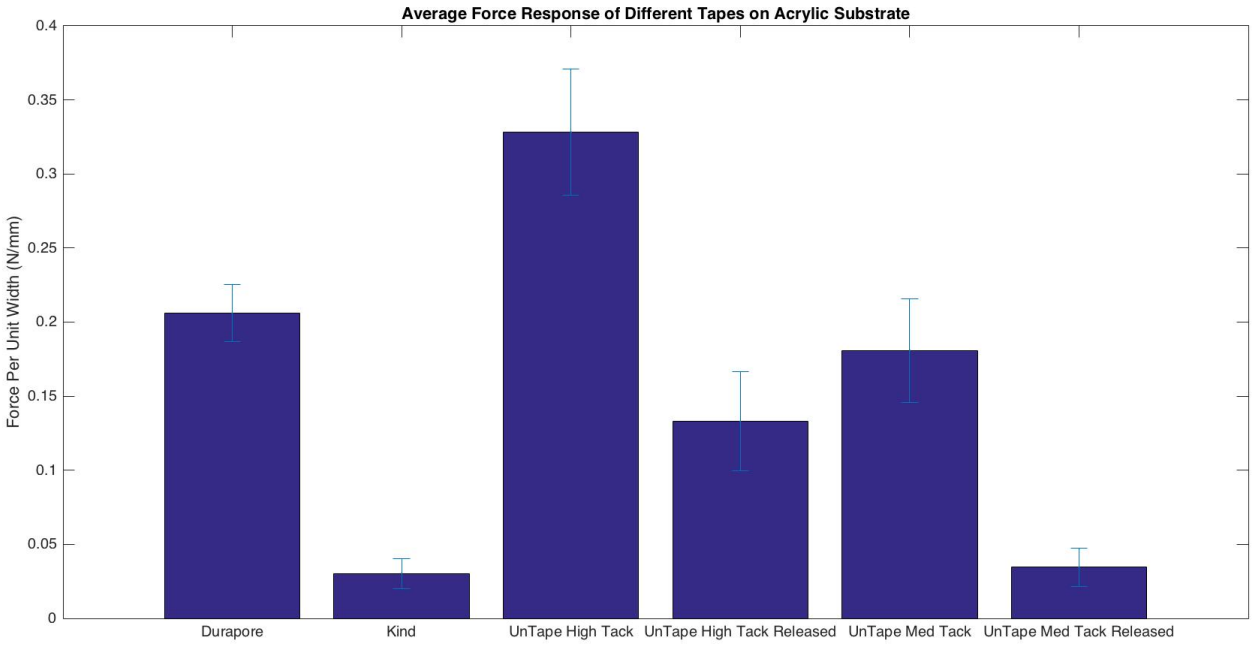

Figure 3.19. Medical Tape Comparisons on Acrylic Substrate

As expected, on both substrates the Durapore tape which is considered to be one of the higher tack tapes used by nurses is much stronger than the Kind tape which is considered to be one of the lowest tack tapes used by nurses. On the stainless-steel substrate, the UnTape high tack tape is stronger than the Durapore before release, and after release is weaker than the kind tape. However, on the acrylic substrate, the UnTape high tack tape after release is much stronger than the Kind tape which makes it difficult to compare. On the stainless-steel substrate, the UnTape medium tack tape is similar to the Durapore before release, and then after release is weaker than the Kind tape. On the acrylic substrate, the UnTape medium tack tape before release is similar to the Durapore, and then after release is similar to the Kind tape as well. However, after doing a student t test to compare the UnTape medium tack before release on stainless steel to Durapore, UnTape medium tack on acrylic before release to Durapore, and UnTape medium

tack on acrylic after release to Kind tape, it turns out that the null hypothesis can be rejected at the 5% level.

Apart from the Kind tape, the other tapes increased their adhesion force by an average of 2.2x in magnitude when transitioning from stainless steel to acrylic. Additional differences in the substrates can be noticed in the residue left on the adhesive portion of the UnTape as shown below in Figure 3.20 & Figure 3.21. Although we gathered data on both stainless steel and acrylic, as mentioned earlier it is difficult to make a leap as to what the expected force values would be on a skin substrate without physically testing it. From testing the stainless steel and acrylic substrates there is a significant difference in the values as we translate from substrate to substrate. However, even with the differences in substrates, the UnTape is still able to achieve significant reduction in adhesion force among both substrates, and there is no evidence to suggest it will not do the same on a skin substrate.

Figure 3.20. UnTape Medium Tack Tape Residue After Acrylic Test

Figure 3.21. UnTape Medium Tack Tape Residue After Stainless Steel Test

3.7 CLEARWELD PRODUCT

In order to make the thermosensitive UnTape photosensitive, and receptible to optical power, we used the Clearweld product [37]. The Clearweld product is a solvent marker which is used to help surfaces absorb light in the near infrared range (NIR). In the case of the Clearweld product used in these experiments, LD920C, the sensitivity of the product peaks in the middle of the 900-1000nm range. For the range of experiments conducted in this paper, high power light emitting diodes (LED's) used were chosen and designed around the sensitivity of the Clearweld product. The specific LED wavelength chosen for all the designs done with Clearweld is 940nm. An image of the Clearweld product used is shown below in Figure 3.22.

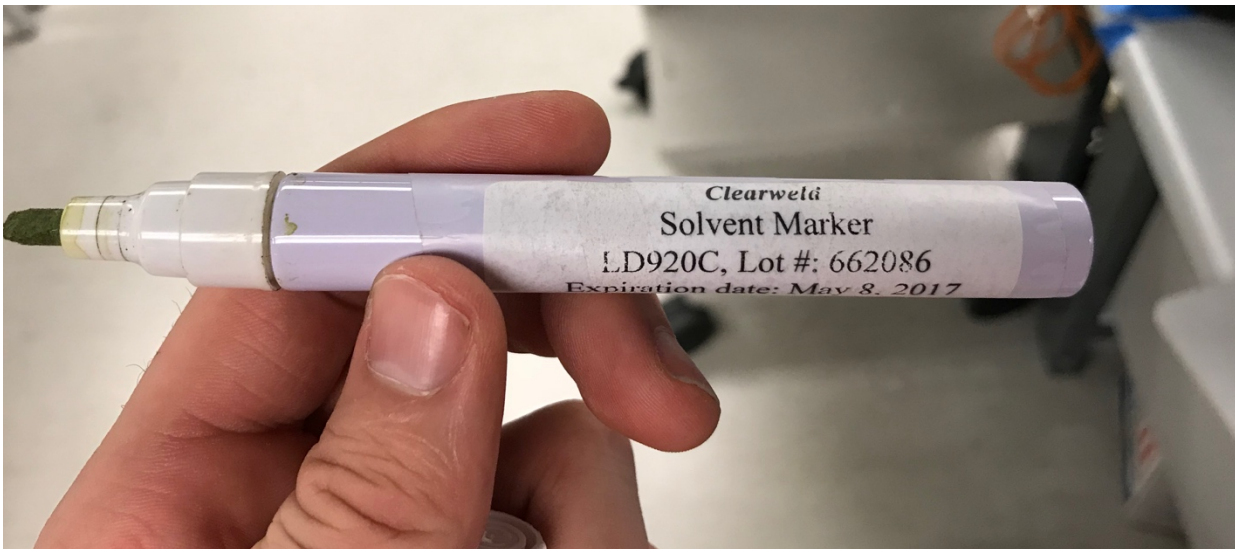

Figure 3.22. Clearweld Product Solvent Marker

In order to use the solvent marker, we simply would draw on the surface of the UnTape backing once we had determined which side had the protective layer. In order to quantify the amount of Clearweld used, we first attempted to measure a difference in mass between amounts of Clearweld applied, however the differences were negligible. We then decided to use different layers as a measurement of how much Clearweld was used. In essence we would color one layer on the tape, wait for it to dry, then add another layer, and so forth. Pictured below are images of four different layering's of Clearweld on the UnTape.

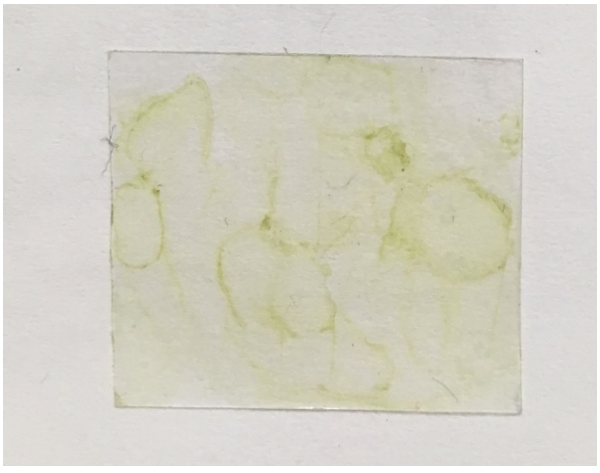

Figure 3.23. UnTape with One Layer of Clearweld

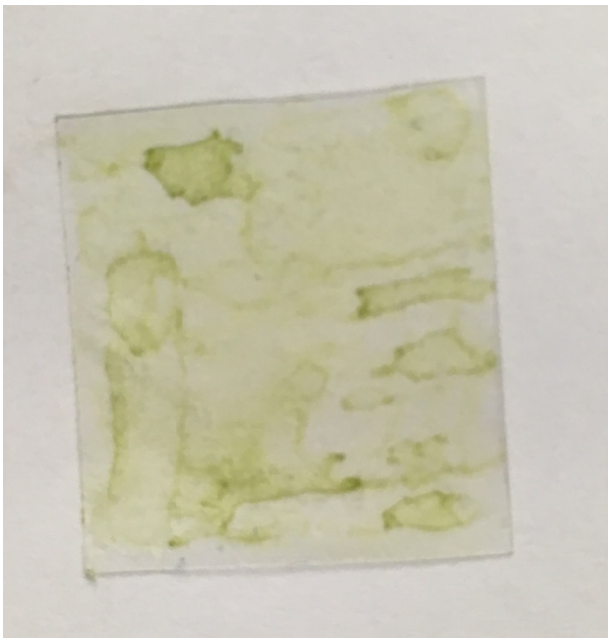

Figure 3.24. UnTape with Two Layers of Clearweld

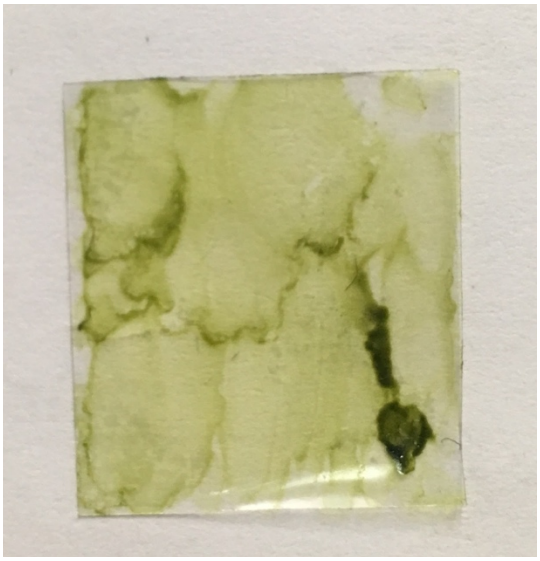

Figure 3.25. UnTape with Three Layers of Clearweld

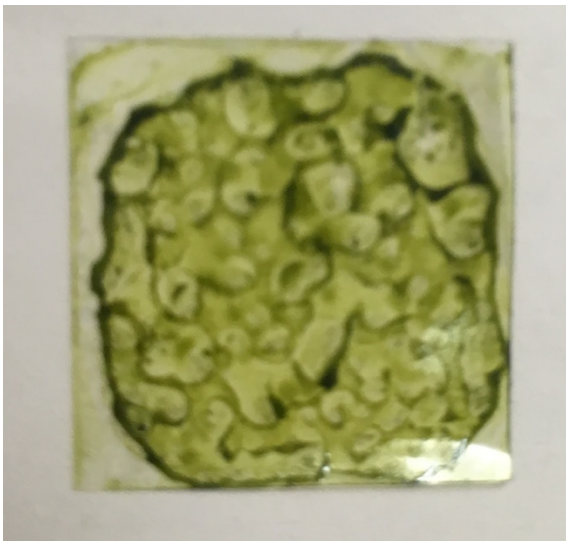

Figure 3.26. UnTape Overcoated with Clearweld

From the four images above, we can see the difference in properties that the Clearweld generates as more layers are added. As more layers are added, the transparency of the tape is reduced, and the thickness of the solvent marker's dye increases. One additional observation of the Clearweld product is that it is seemingly hydrophobic to the UnTape surface as compared to other tapes tested on. This can be described by observing the non-uniformity of the distribution of the dye on each of the figures, and most noticeably on Figure 3.26. In order to further explore the differences in adding layers of Clearweld, we tested the light transmission through the tape. In order to examine the transmission, we used Ocean Optics Spectrasuite hardware & software. An image of the setup is shown below in Figure 3.27, along with the baseline control measurement in Figure 3.28, one layer light transmission in Figure 3.29, and two layer light transmission in Figure 3.30.

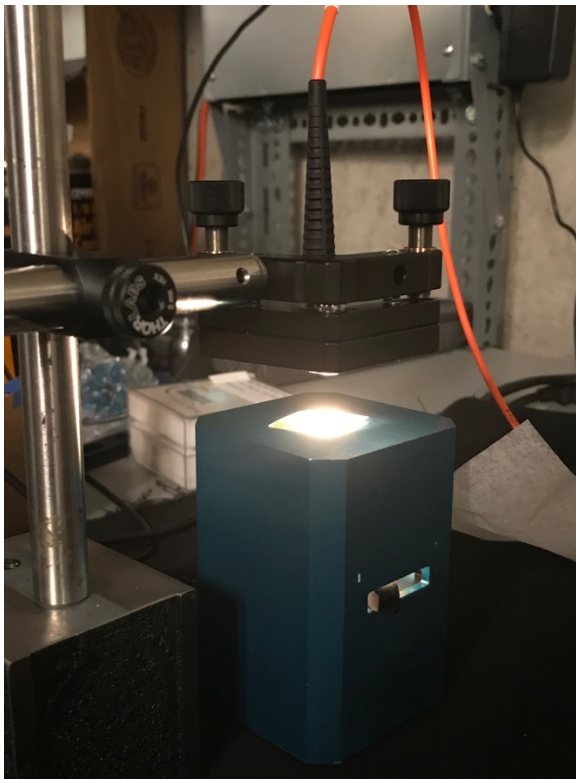

Figure 3.27. UnTape Light Transmission Test

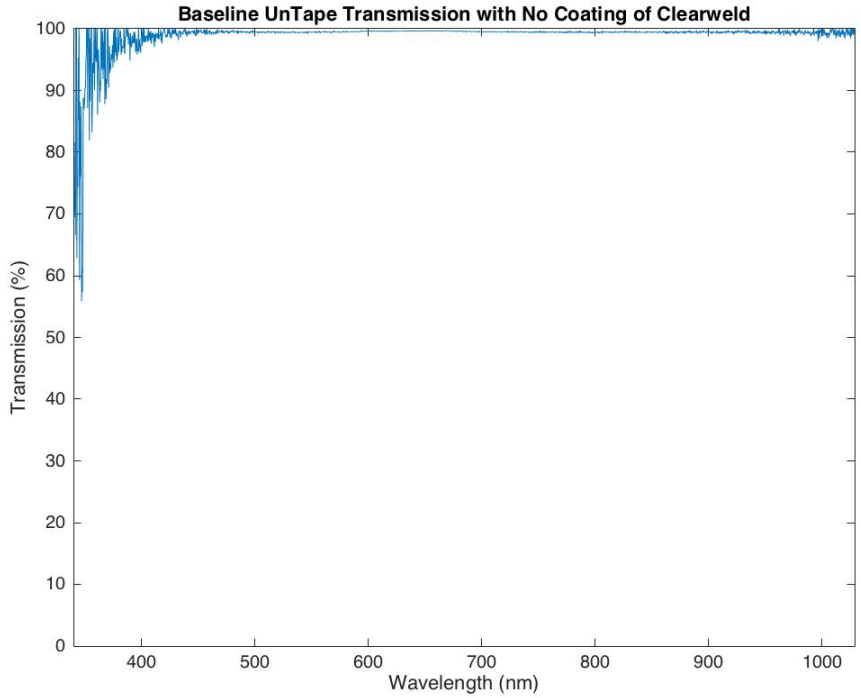

Figure 3.28. Baseline Transmission Measurement on UnTape for no Clearweld

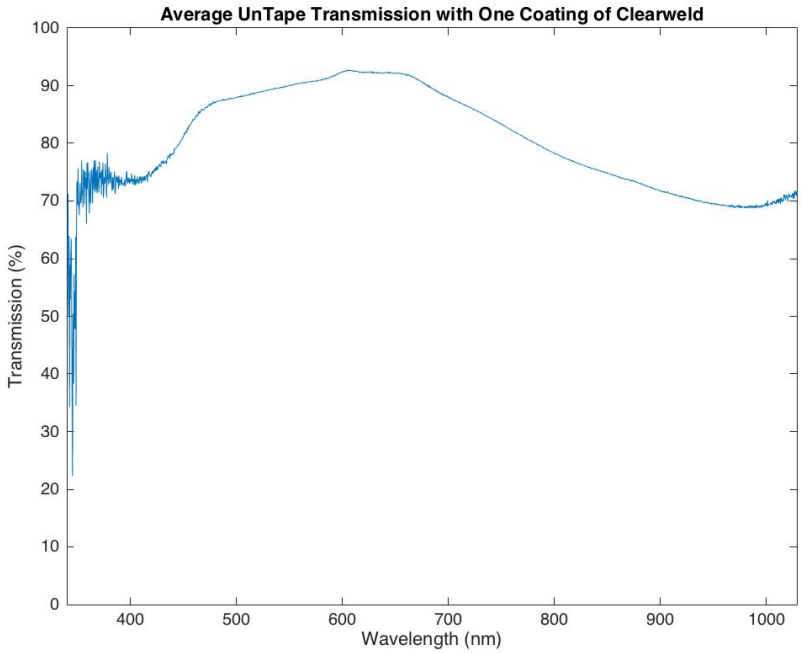

Figure 3.29. Transmission on UnTape with One Layer of Clearweld

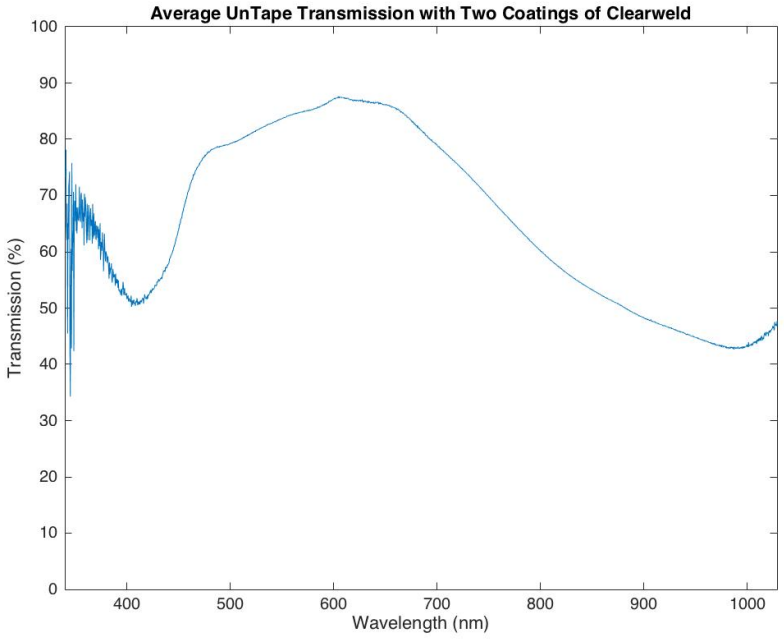

Figure 3.30. Transmission on UnTape with Two Layers of Clearweld

Data collected in these tests was gathered with random sampling around the domain of the UnTape in both the one and two-layer case. The tape was moved around in 20 different positions for each case to try and account for the non-uniformity of the Clearweld product. The baseline test (no Clearweld) had a 99.45% transmission with a standard deviation of .172%, the one-layer UnTape had a transmission of 69.86% with a standard deviation of 3.11%, and the two layer UnTape had a transmission of 45.47% with a standard deviation of 6.82%. The results of this test show that as we add more layers of Clearweld product to the UnTape, the absorption of the light energy will increase. Additionally, the non-uniformity caused by the hydrophobic properties of the UnTape surface can be quantified by the increase in the standard deviation from the baseline measurement to the one-layer UnTape, and then again to the two-layer UnTape.

In order to further test the photo-absorption ability of the Clearweld, we took the four differently soiled tapes from Figure 3.23– Figure 3.26 and used our original LED wand described in Section 5.1 & Figure 5.1 to measure the rise times for the different pieces of tape. In order to collect the data in this experiment we placed the tapes on an acrylic substrate and attached a small thermocouple below the tape. We set up a video camera to monitor the temperature change of the thermocouple and then applied the LED wand just above the surface of the tape and measured the thermal response which is shown below in Figure 3.31. From our tests we were able to show that as we increase the layers of Clearweld, the temperature rise time decreases as well. This also suggests that the light transmission tests done in Figure 3.27 & Figure 3.30 are an important factor to account for the difference in temperature rise times observed. When there is less light transmission the temperature rise time will decrease, however in the case of the over-coated tape, it seems that the Clearweld product saturated and lost effect.

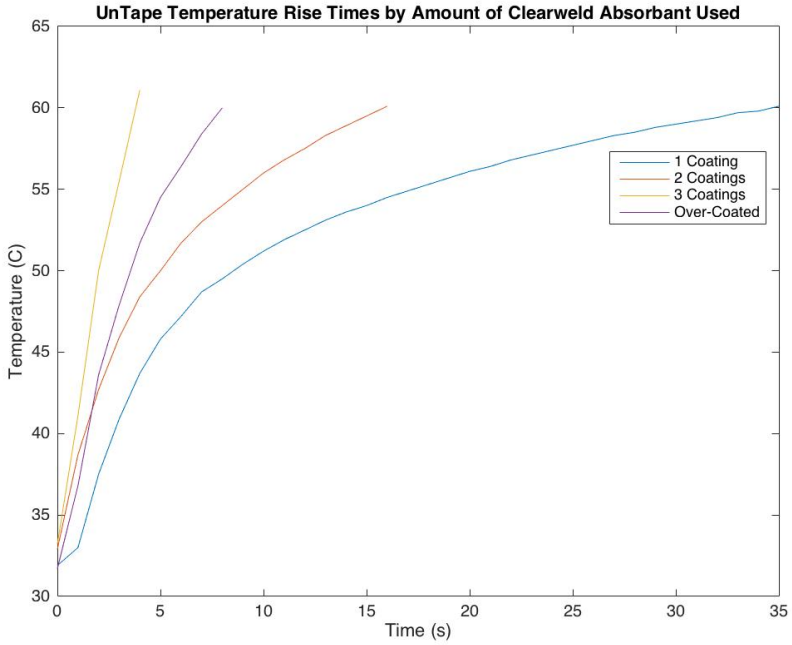

Figure 3.31. UnTape Temperature Rise Times by Layers of Clearweld

Chapter 4. MODELING

4.1 1D Finite Element Model

After characterizing the UnTape peel adhesion strength before and after thermal activation, the next goal was to measure the transient heat transfer into the tape. We had already established we can drop the peel adhesion force substantially if we dump a bunch of energy into the tape, however what we didn't know was the transient temperature profile of the tape and that of the substrate below it.

In order to test this, we adhered a piece of UnTape to skin and placed a thermocouple in-between the tape and skin. We then heated up the UnTape with our first LED wand described in Figure 5.1 and recorded the temperature change shown on the temperature controller output of the thermocouple. A 1D Finite Element heat transfer model was created in Matlab and matched to the skin curves generated from the test using skin and flesh properties mentioned in Section 3.1. The model was created with the assumption that during the heating of the tape, conduction is present but convection is assumed to be negligent due to the wand being almost in contact with the tape, as well as irradiation. Once the wand is removed, the input heat source is turned off and convection is turned on. The thickness of the skin & flesh is assumed to be 10 mm and tape 1 mm. The heat transfer model results are shown below, where each line on the graph corresponds to a node in the model, and then the tape surface node is also shown in comparison to the observed trials of temperature rise and decay done on human skin in Figure 4.2.

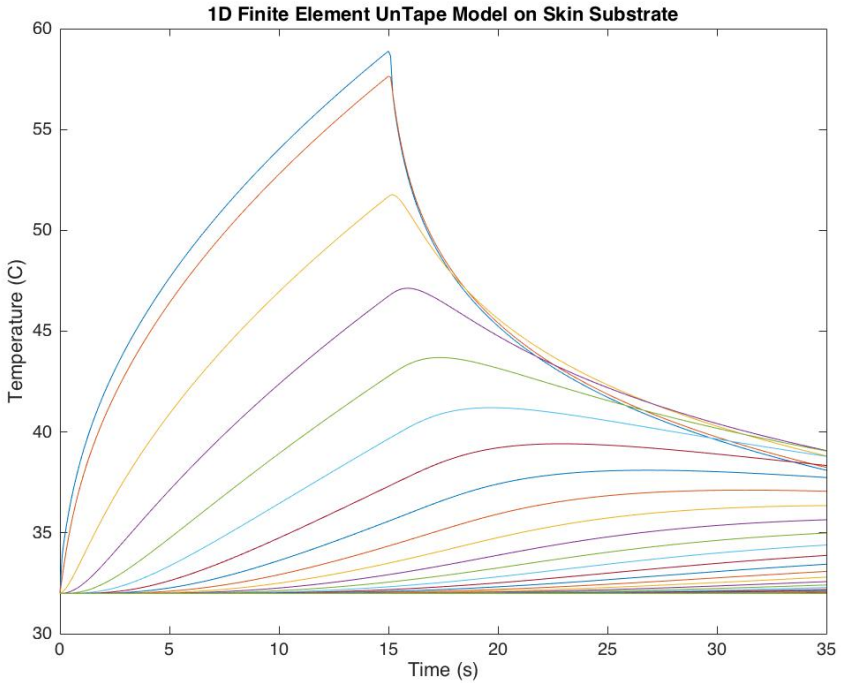

Figure 4.1. 1D Finite Element UnTape Model on Skin Substrate

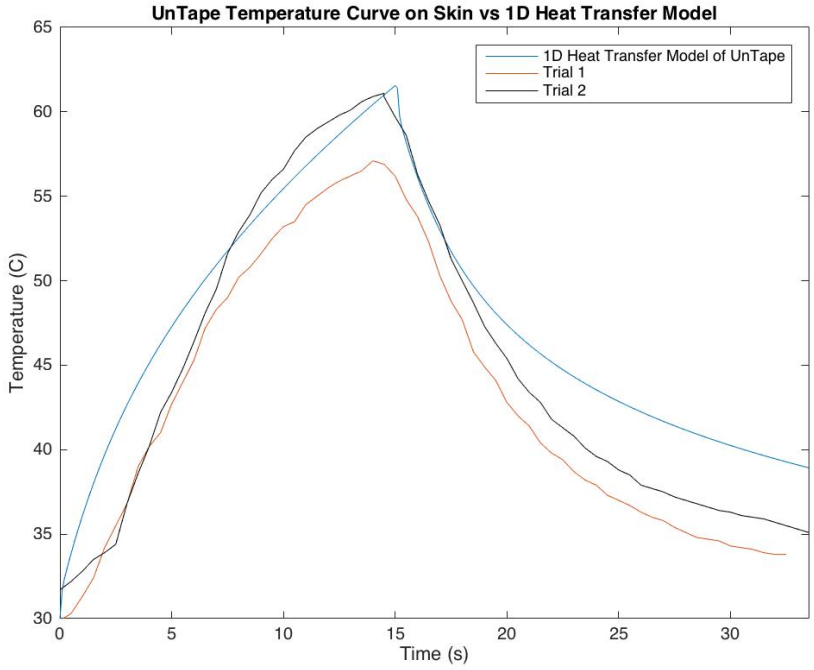

Figure 4.2. UnTape Skin Temperature Compared to 1D F.E. Heat Transfer Model

For the optical power source used, the transient temperature rise profile and decay profile of skin seems to be similar to the theoretical values computed from the 1D finite element model processed in Matlab, which gives validity to the referenced values in Section 3.1. The differences among the temperature profiles in both trials is likely due to the non-uniformity of the output of the LED wand, however the general trend is followed.

4.2 COMSOL MULTIPHYSICS MODEL

With the validity of the 1D finite element model previously shown, it was then desired to make 2D models to better understand the transient physics of heat transfer in our system, and the critical areas to worry about on skin. We used Comsol Multiphysics to populate the heat transfer models of skin and acrylic to match the results gathered from the PID testing with known inputs. Unlike the 1D heat transfer model created in Matlab, this testing was done with an updated wand therefore several assumptions were changed. Since the UnTape wand is designed to be non-contact and is the window is located approximately 10-15 mm from the skin, both convection and irradiation are not considered to be negligible. The values for emissivity for skin and acrylic used were .95 and .94 respectively [30]. Since Clearweld has no data on emissivity, the tape was assumed have the emissivity of acrylic, since it is an acrylate-based tape. The models were created with the UnTape placed on top of a block of variable substrate, being either skin or acrylic. Shown below are the 2D model results created with skin and acrylic substrates.

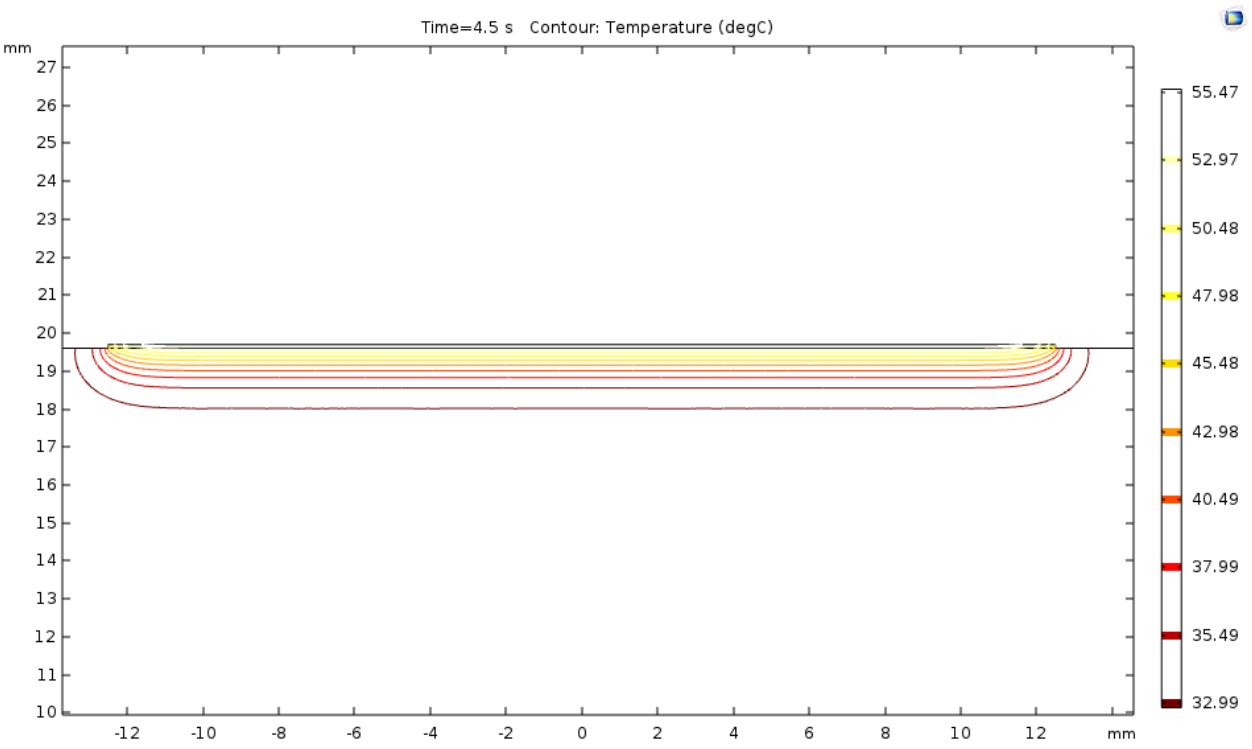

Figure 4.3. 2D Comsol Model for UnTape Wand Rise Time on Acrylic Substrate

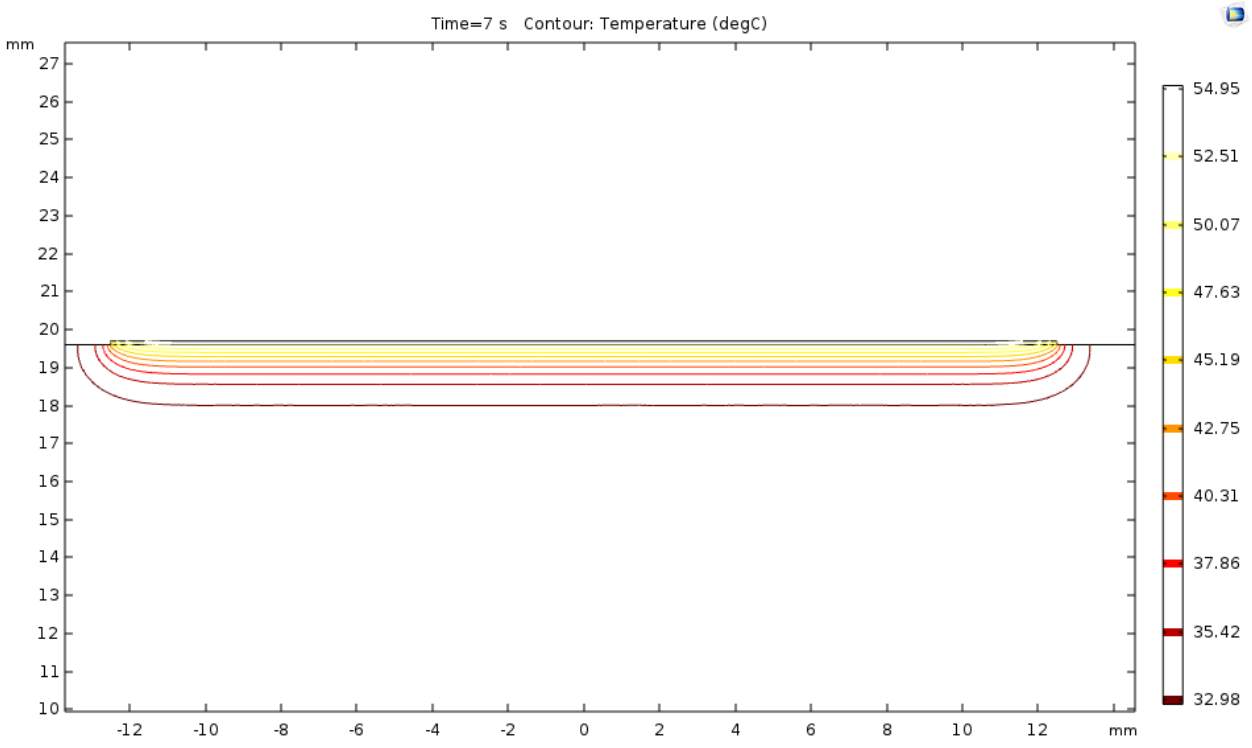

Figure 4.4. 2D Comsol Model for UnTape Wand Rise Time on Skin Substrate

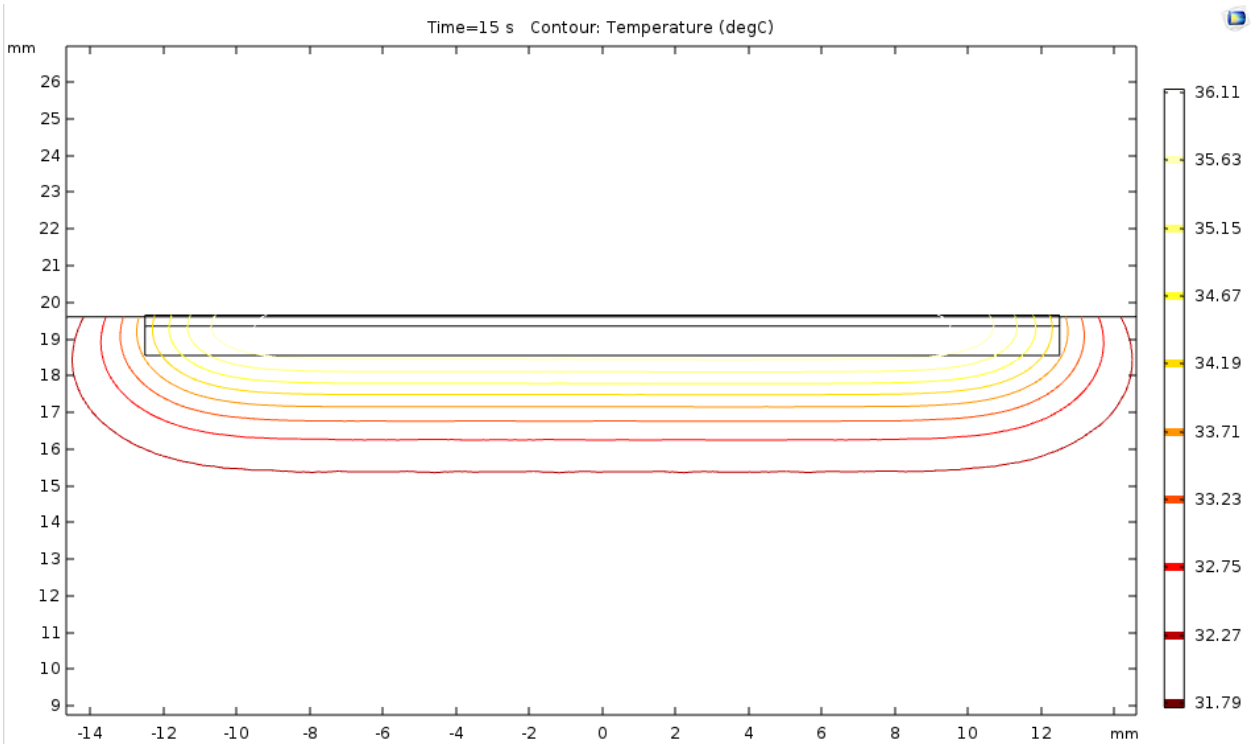

Figure 4.5. 2D Comsol Model for Acrylic Substrate Cool Down

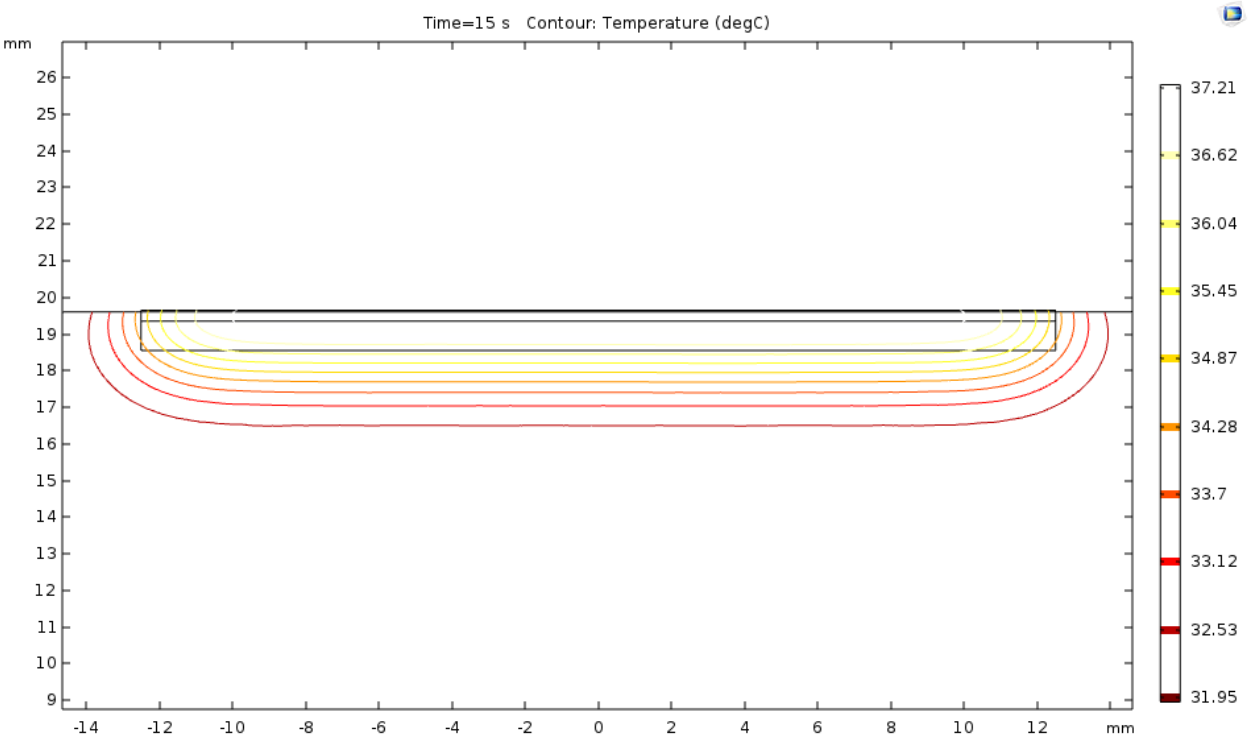

Figure 4.6. 2D Comsol Model for Skin Substrate Cool Down

From these models, it is apparent that both skin and acrylic substrates are related in terms of their transient response to thermal change. Both materials heat up at a similar rate, however skin seems to heat up at a slightly slower rate, and also dissipates heat slightly slower than our acrylic substrate. This result means that we know that skin data will never exceed or surpass the results gathered using acrylic. Exporting all of the 2D data into Matlab and populating nodal temperature lines for skin, we receive the following plot.

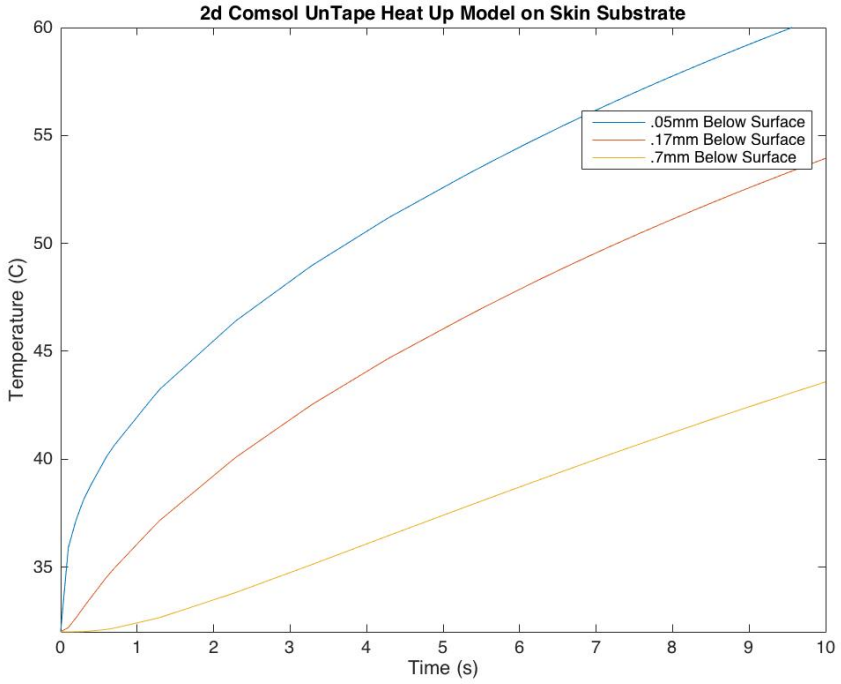

Figure 4.7. 2D Comsol Model for UnTape Wand Rise Time on Skin Substrate

The different lines referenced in the plot above correspond to different nodes in the skin contour temperature plot shown in Fig 18. The first node is approximately at the tape surface, the second chosen node is .17mm below the surface of the skin, and the last node is .7mm below the surface of the skin. From this data we can extrapolate that the majority of the heat transfer occurs in the top 1mm chunk of volume in the skin and dissipates extremely quickly. From Figure 4.3 - Figure 4.6, there is an apparent lag time between the transient temperature rise of the skin and

acrylic substrates. The lag time is approximately 3.5 s at 55 C°, and then .5 s at 45 C°. Although the two substrates are not identical in terms of heat transfer, the acrylic substrate can be used to have a general idea of what will happen on a skin substrate, thermally. Comparing the UnTape surface node transient data for both substrates we receive the following plots Figure 4.8 & Figure 4.9.

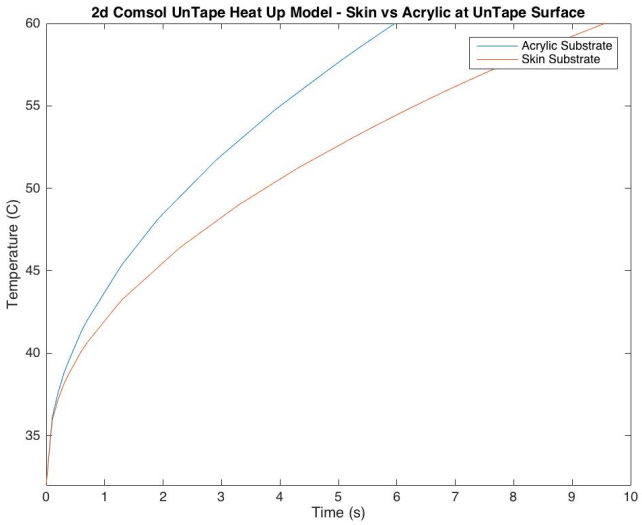

Figure 4.8. 2D Comsol UnTape Heat Up Model – Skin vs Acrylic at UnTape Surface

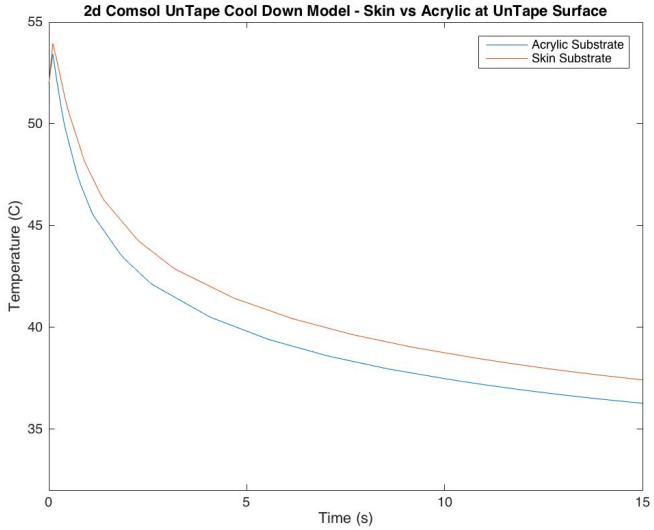

Figure 4.9. 2D Comsol UnTape Cool Down Model – Skin vs Acrylic at UnTape Surface

Chapter 5. WAND DEVELOPMENT

5.1 Light Emitting Diode (LED) Board

In order to take advantage of the thermosentive and photosensitive properties of the UnTape, we needed a method to activate the heat transfer. In order accomplish this goal it was decided to use high power light emitting diodes (LED's), taking advantage of the photosensitive properties of the Clearweld product described in Section 3.7 to ramp the temperature up to the adhesion transition range. The LED wavelength in question used for all experiments done in this paper was 940nm. The first LED configuration that was tried was an LZ4-00R708 LED produced by Led Engin. At a current of 1180mA, the LED produces 5.9W of optical power while consuming approximately 12.0W of power which gives an efficiency of approximately 49.2%. An image of this LED is shown below in Figure 5.1.

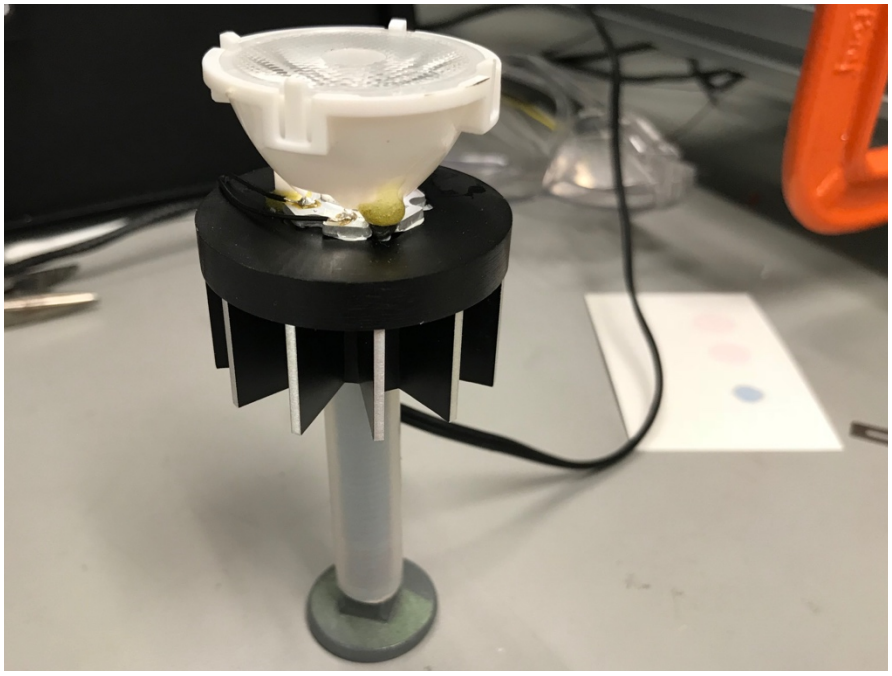

Figure 5.1. LZ4-00R708 LED Wand

Due to the high-power requirement and efficiency rating of the LZ4-00R708 LED, we attached a large heat sink to the back of the LED. In order to be able to control the position and movement of the LED without having to physically be in contact with the LED we added a shaft with tubing around it to attempt to not only give somewhere to grip the wand, but also to insulate the heat transfer in the shaft the tubing. On top of the LED is a hemisphere window responsible for making the optical power distribution diffuse and add more uniformity. This was the first LED wand used for several tests.

However, due to the size of the LED, the half angle of exit, and the size of the heat sinking required to dissipate heat, it was desired to find smaller LED's with smaller half angles of exit so that the optical power is more concentrated. The next LED which was tested was a SFH 4248 LED-VAW LED produced by OSRAM. The LED had a much smaller exit half angle of 15°. Before creating a customized printed circuit board (PCB) we needed to be able to know the optical power distribution and know that we were receiving an even distribution.

In order to fulfill this requirement, we created a Matlab program capable of taking the specifications of the LED and creating a plot of the optical power distribution depending on the desired orientation of the LED's. What the program does is that it takes into account the half angle of the LED and creates a distribution. With this distribution we can then combine different numbers of LED's, individual positions of LED's and generate distribution plots of the optical power. From here the effective power and efficiency of the LED's can be calculated depending on the distance from the UnTape. Shown below is the optical power distribution of the SFH 4248 LED-VAW LED orientated with 3 parallel branches of 5 LED's offset and skewed by 2 mm in each row.

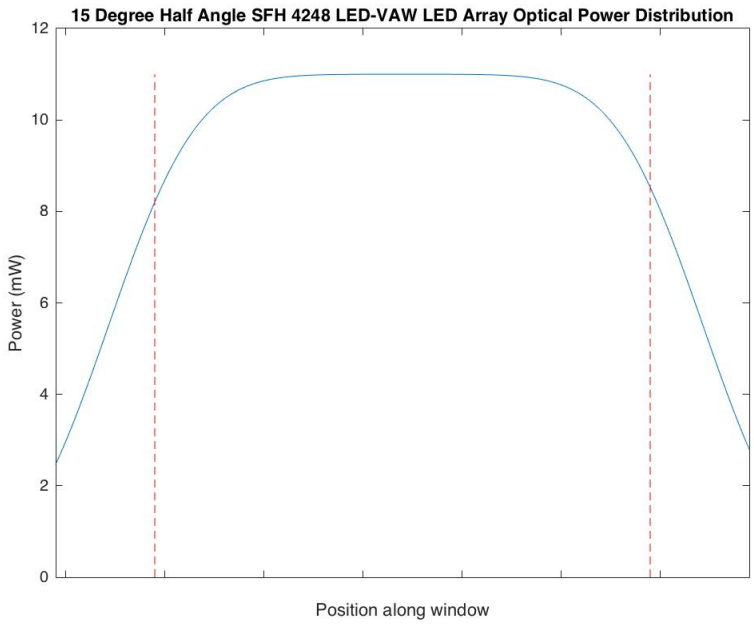

Figure 5.2. SFH 4248 LED-VAW Power Distribution

The graph above shows the optical power distribution of the SFH 4248 LED-VAW LED. The label of the x axis "position along window" refers to the wand casing that was being created simultaneously to designing the LED array. The red lines symbolize the domain of the area where the UnTape will be exposed by the wand. In order to find the effective optical power, we integrate the power across the domain of the window. Once this was completed the next step was to design an LED board for the configuration used in the optical power distribution program. We used ExpressPCB in order to design and order the board. As described earlier, the LED board was created with three different parallel branches skewed in space, with each branch containing LED's in series. The reason for separating the LED's into parallel branches was to make sure there was no power drop off from LED to LED due to having too many LED's in series. The board is shown below in Figure 5.3 & Figure 5.4.

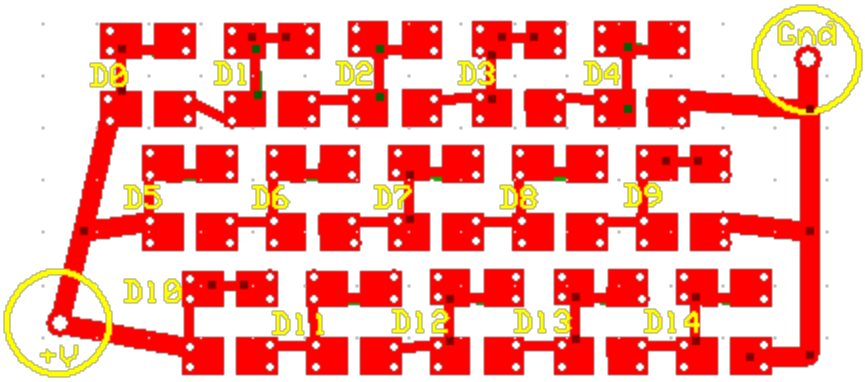

Figure 5.3. SFH 4248 LED-VAW LED Array Design

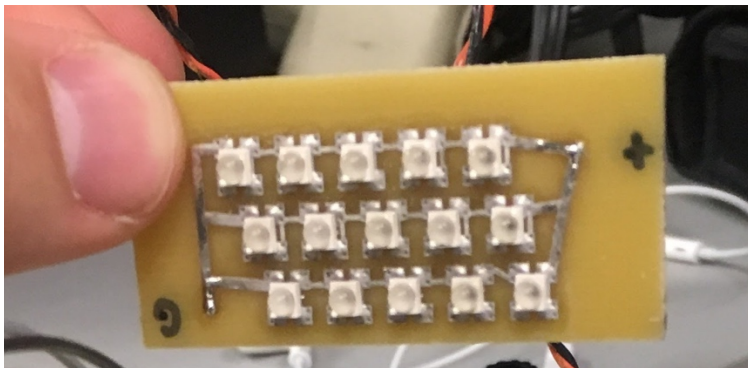

Figure 5.4. SFH 4248 LED-VAW LED Array Assembled

After creating the SFH 4248 LED-VAW LED array, we tested the board but we received very little power output and transient temperature change in the UnTape. We then realized that there was a miscalculation made with the steradian angle and its relation to the power generated in the board, meaning that we had poorly chosen the LED's and needed to restart the design. After redoing the calculations and searching for different LED's we settled with a Lumiled L1I0-0940060000000 LED [38] which has a much higher power output than the previous LED used. However, with a higher power output, the evenness of the optical power distribution is sacrificed. The optical power distribution, PCB design, and LED array are picture below in Figure 5.5 - Figure 5.7.

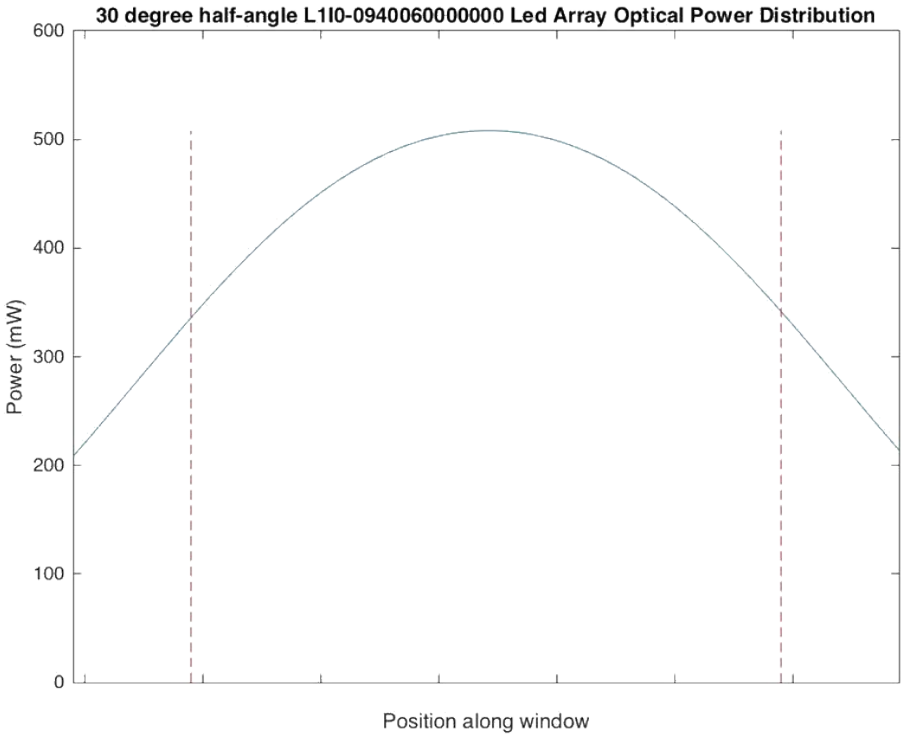

Figure 5.5. Lumiled LED Array Optical Power Distribution

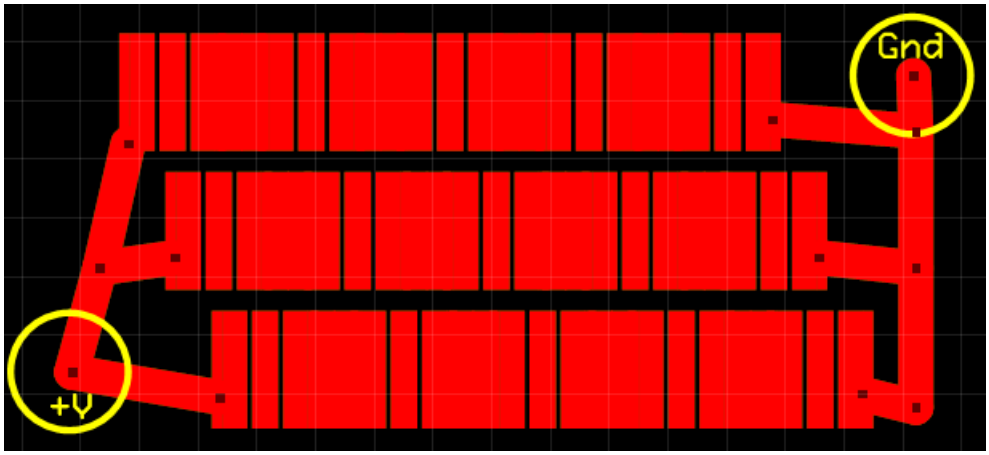

Figure 5.6. Lumiled LED Array Design

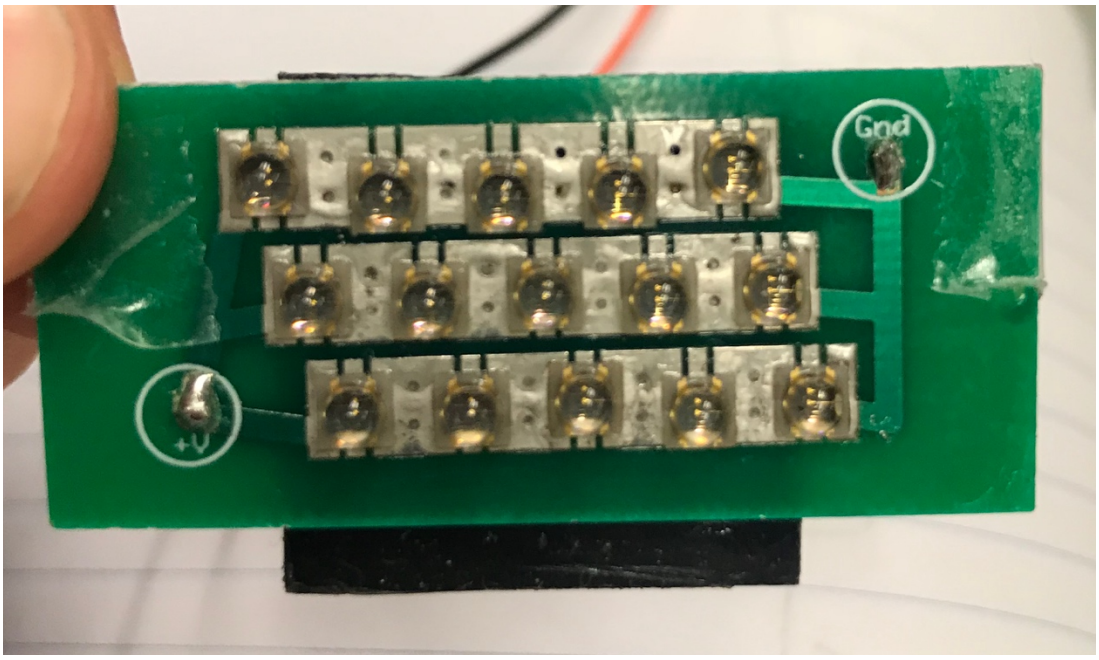

Figure 5.7. Lumiled LED Array Assembled

Compared to the SFH 4248 LED-VAW LED which outputted approximately 264.8mW of optical power at its maximum rated current, under this design the Lumiled array outputs approximately 11291mW at full power which is factors of magnitude larger than the previous incorrect design.

5.2 Arduino/LED Driver Board

With the LED board created, we needed to be able to have a way to control all of the different components on the board. We decided to use an Arduino Nano to modulate and control the different components on the board due to its simplicity of use. The first component that needed to be controlled was the LED board. We needed to be able to control the power output of the board, as well as be able to send enough current to the board in order to power it. Since we want to control the power of the board such that we don't overshoot a temperature setpoint and burn a patient, we used a non-contact infrared temperature sensor to measure the temperature of what is in front of the UnTape wand. Since the output current of the Arduino Nano is relatively

small compared to the required current of the LED board, we created an LED driver that pulled from an outside power source to power the LED board. Additionally, we wanted to have an exterior indication of the temperature of the UnTape, so an RGB LED was added to the Arduino board. An image of the Arduino/LED driver board without components is shown below in Figure 5.8.

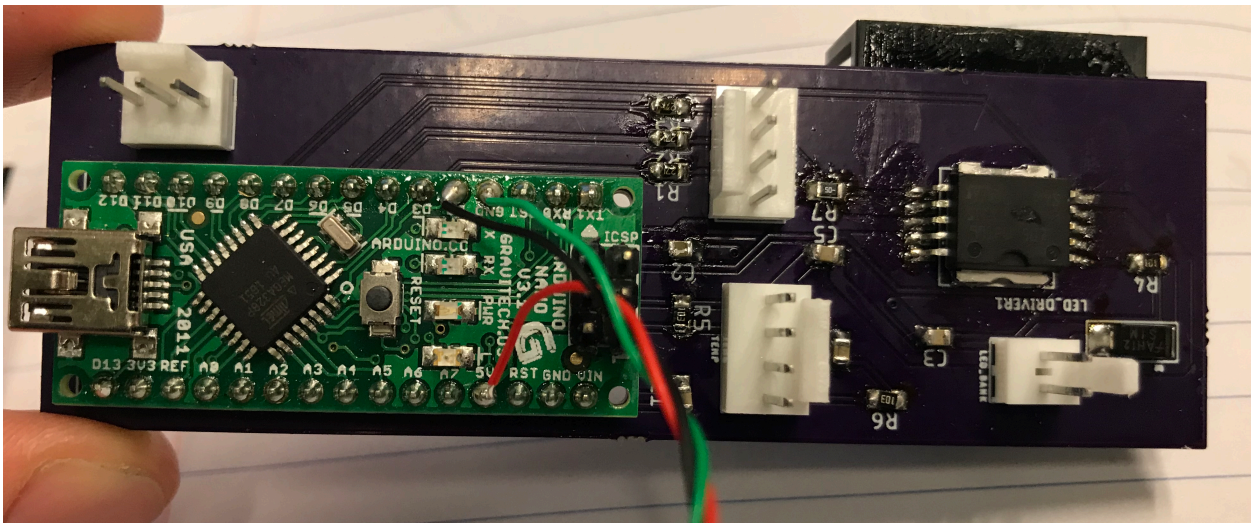

Figure 5.8. Arduino/LED Driver Board

The Arduino board pictured above contains the different components described previously: Arduino Nano, pins for an exterior power source, pins for LED array, pins for RGB LED, pins for the non-contact infrared temperature sensor, and the LED driver chip. Due to the high current requirement of the LED board, the LED driver dissipates a lot of heat, so we placed a heat sink behind the PCB, and a fan behind the heat sink to help reduce the heat transfer on the chip and prevent it from overheating and saturating. In order to get all of the components to work together, an Arduino program was created to drive the entire system. What the program does is that it takes the input of the non-contact infrared temperature sensor and compares it to the desired setpoint, which in our case is 55C°. The Arduino then uses a tuned PID controller to output a pulse width modulation (PWM) signal to drive the LED driver which amplifies that

signal to a current that powers the LED board. Once the temperature of the tape reaches the setpoint, the PID then keeps the tape stationary at the setpoint. Additionally, depending on the temperature measurement of the non-contact infrared temperature sensor, the RGB LED will display either red, green or blue to signify the temperature range of the tape. In the case of this program, the light would be green up until 40C°, then blue from 40 to 55C°, and finally red from 55C° onwards. In order to test the PID system of the Arduino and its ability to control and modulate the LED board, we set up a similar test system to the orientation of the UnTape wand design, with the UnTape adhered to an acrylic substrate used. This setup is shown below in Figure 5.9, and a temperature rise time shown in Figure 5.10.

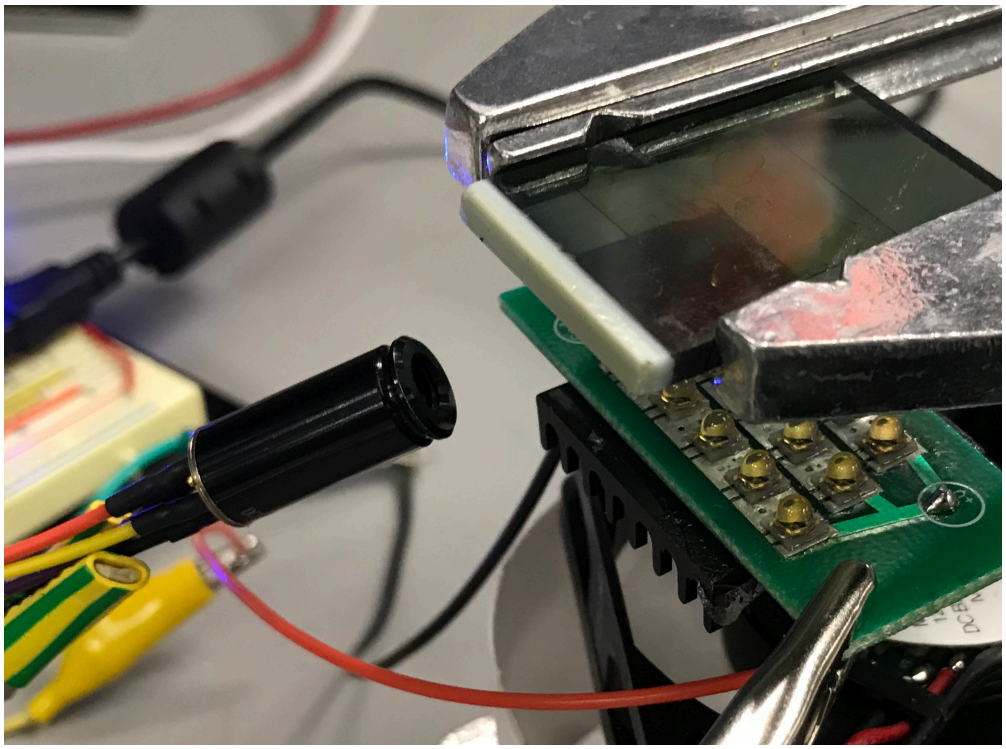

Figure 5.9. PID Testing System with LED Board, UnTape on Acrylic, and Sensor

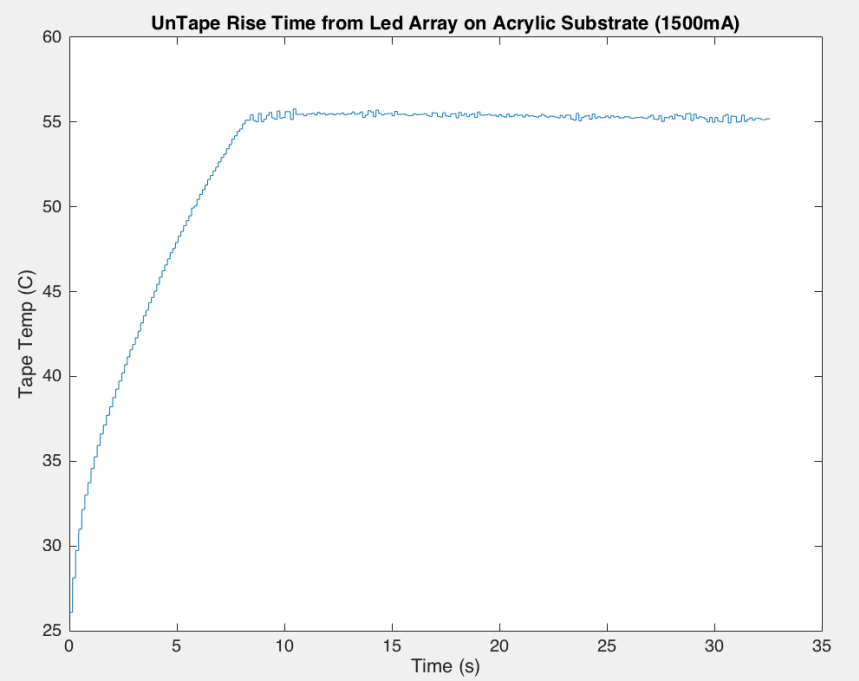

Figure 5.10. Example Temperature Rise Time & PID Control

The average variation or overshoot by the tuned PID controller once it hit the setpoint of 55C° was .48C°. We then tested an assortment of different currents, ideally, we wanted to get from normal skin temperature to 55C° in approximately 5 seconds. We tested 1500mA, 2000mA, and 2500mA current inputs on two different samples of UnTape, one coated with one layer, and the second coated with two layers. With one layer, the temperature rise times are extremely slow, and even at 2500mA, the rise time is still higher than the desired 5 second window. In the two-layer testing, the rise times are much quicker due to the higher light absorption. From the plots below, we knew we needed to set the LED driver to output a current between 1500mA and 2000mA and use a tape coated with at least two layers. The rise times for these scenarios are showed below in Figure 5.11 & Figure 5.12.

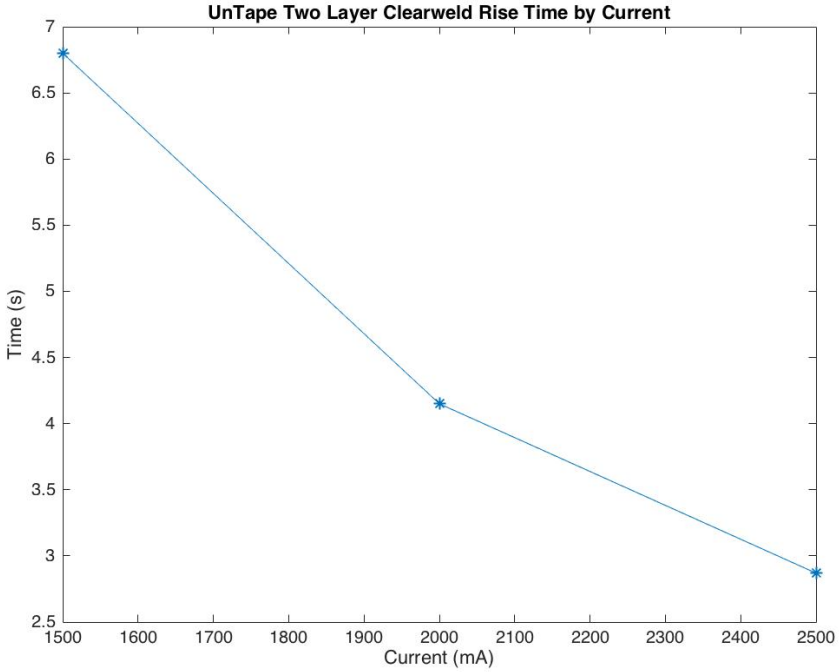

Figure 5.11. UnTape Two-Layer Clearweld Rise Times by Current

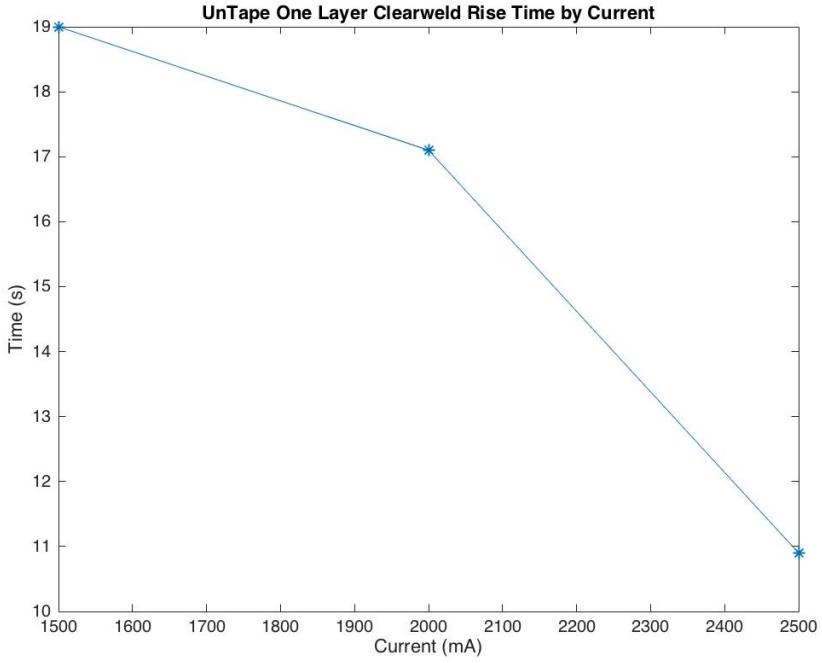

Figure 5.12. UnTape One-Layer Clearweld Rise Times by Current

5.3 Additional Components

The last few components of the wand are a non-contact temperature sensor, a window, and a button. As described in Section 5.2, we needed a way to measure the temperature of the UnTape, and in order for the UnTape wand to be portable, the temperature measurement device needed to be non-contact. We decided to use a Melexis MLX90614xCI sensor [31] which has an extremely narrow viewing region with a half angle of 2.5°. This small viewing angle is important which because that meant it would still read relatively small areas on tape from far away. In order to test the accuracy of the Melexis non-contact infrared sensor, we needed to measure it against an accurate temperature source. We used a Neslab Chiller, which is a device used primarily for cooling, however can be used to heat up as well. In the Neslab Chiller there is a rectangular volume which can be filled with water, and when turned on the chiller circulates the water continuously through its internal system and takes temperature measurements. Since the walls of the Neslab Chiller are metal, we placed a black plastic block near the surface of the circulating water to take measurements from. For each temperature interval, we waited an additional 30 minutes for the block to reach the steady state temperature of the chiller before taking measurements with the Melexis temperature sensor. Pictured below are the Neslab Chiller and the data received from comparing the Neslab Chiller to the Melexis sensor in Figure 5.13 & Figure 5.14.

Figure 5.13. Neslab Chiller

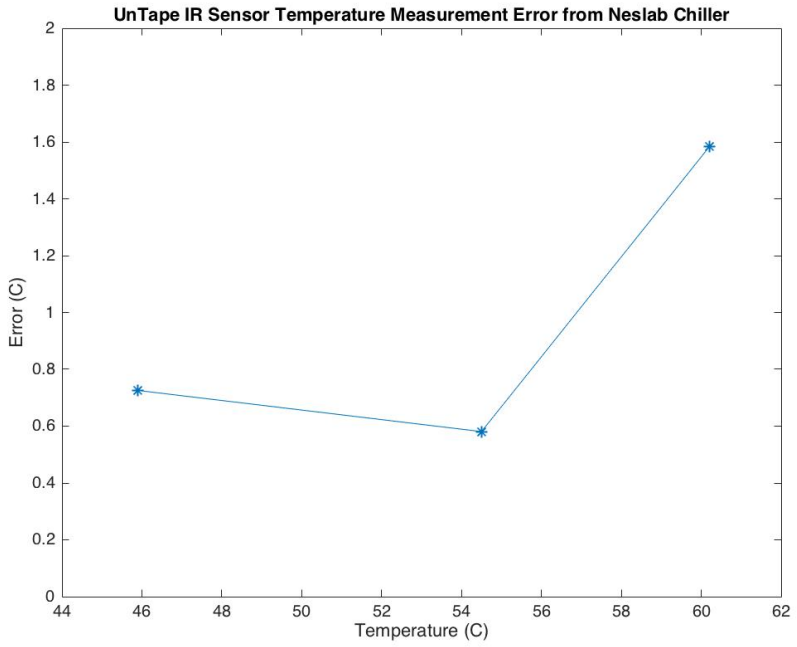

Figure 5.14. Melexis Sensor Error from Neslab Chiller

On average, there was an error of .96 C° between the non-contact infrared temperature sensor and the Neslab Chiller. This error can be caused by a number of things, such as the fact that the plastic block was located near the surface of the water, and since the Neslab Chiller circulates and measures water near the middle of the volume, the temperature at the top of the water would be slightly different. Another possible reason is due to the emissivity of the block since we are dealing the infrared readings, and the final possible reason is that the block is not completely reaching the steady state temperature. However, we were able to show that the temperature sensor which we possess is calibrated within a close range of calibrated temperature values.

The last portion of the design was to have a window shielding the LED board from the surface of the UnTape and skin. A window was required because the LEDs require a path of view to the UnTape. If we have an opening in front of the UnTape wand, we could allow junk to come inside the device, as well as potentially cause harm to a patient with discomfort from coming in contact with corners. Initially we settled on a polycarbonate window, because polycarbonate is transmissive of infrared light [29]. We tested the window and it was transmissive of the LED board, however we could not get readings with the non-contact infrared temperature sensor. This is because the polycarbonate is transmissive upwards of 90% in the near infrared range (700 nm – 1000 nm), however is not very transmissive in the infrared range (1000 nm – upwards). In the case of the temperature sensor we have, the range of the sensor was from 5500 nm to 14000 nm [31] so it caused the sensor to only read the temperature of the window's internal surface. We then switched to a sodium chloride window which is transmissive upwards of 90% [30] in both the NIR and IR range, and tested the accuracy of the sensor. We tested it on a black material substrate with temperatures ranging from 30C° to 60C°, with and

without the sodium chloride window positioned in front of the temperature sensor's view. With the correction factor used, there is approximately an error of 1.23C° when using the sodium chloride window as compared to when not using the sodium chloride window in front of the temperature sensor. The data for this experiment is shown below in Figure 5.15.

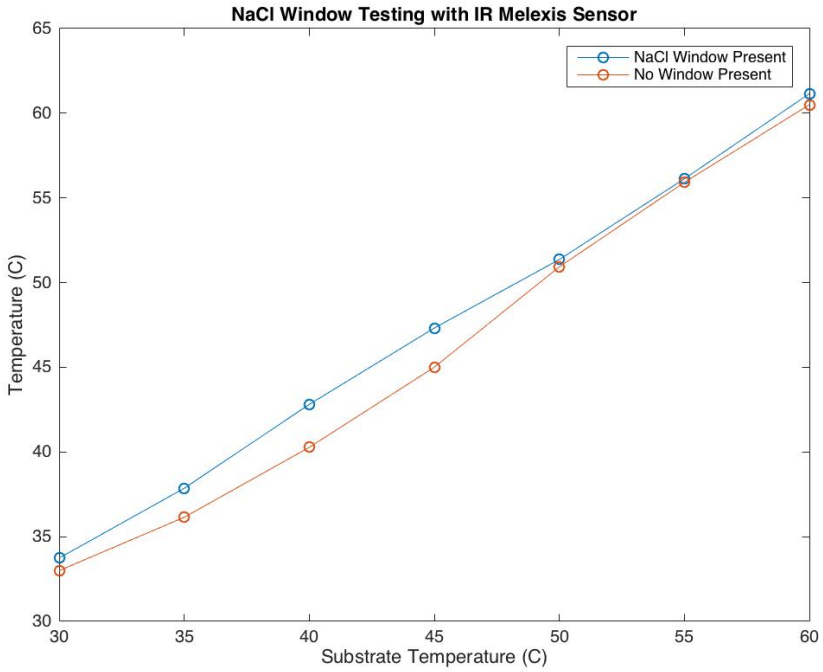

Figure 5.15. NaCl Window Testing with IR Melexis Sensor

5.4 WAND BUILDS

The wand designs were created in Solidworks and progressed simultaneously to the different components described in the previous sections of Chapter 5. All wand prototypes were 3D printed with PLA filament due to their high melting points, making it useful for applications involving temperature fluctuation. The first-generation wand was made with the idea of trying to primarily fit the LED board and non-contact infrared temperature sensor in. Pieces of the part and assembly are shown below in Figure 5.16 - Figure 5.18.

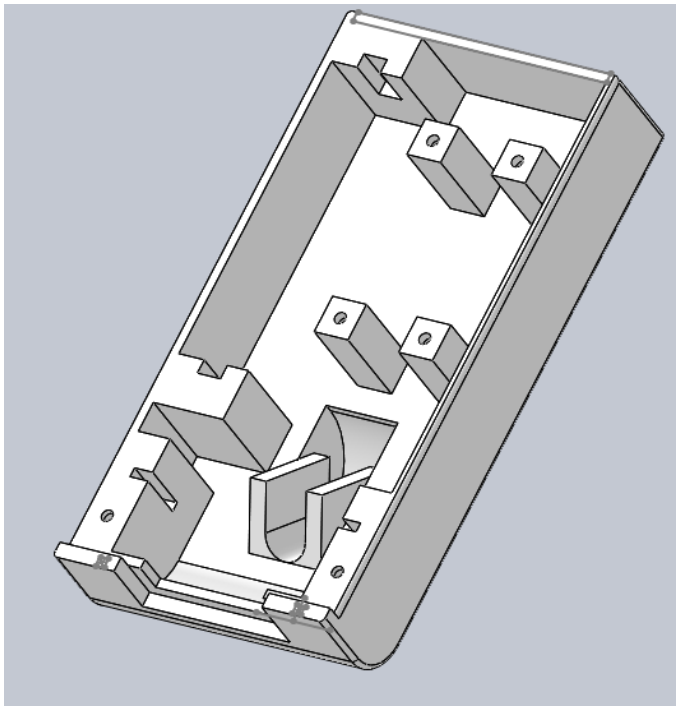

Figure 5.16. UnTape Wand 1st Gen Top Section

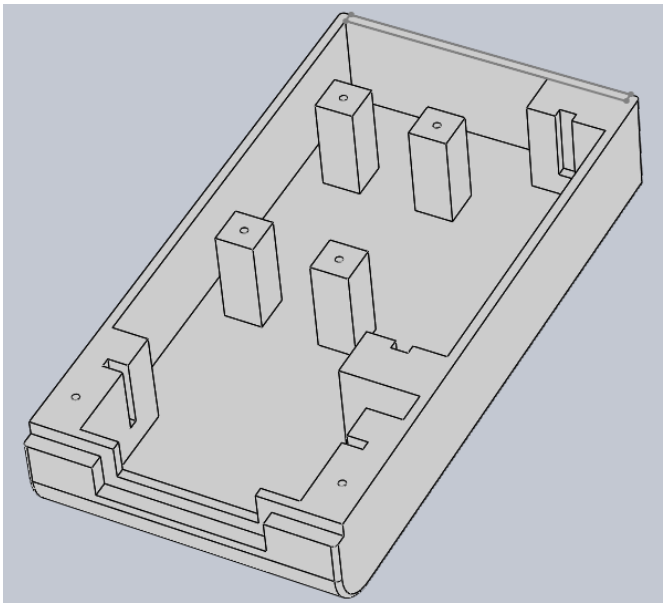

Figure 5.17. UnTape Wand 1st Gen Bottom Section

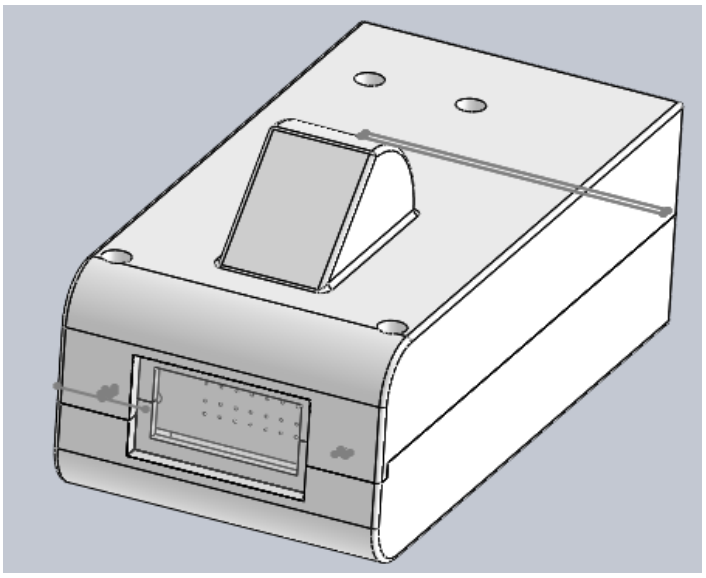

Figure 5.18. UnTape Wand 1st Gen Assembly

The top portion of the wand has a slot for the Arduino/LED driver board in the top left of the image, and slots for the LED board near the open window are located near the front of the wand. The slots for the LED board are positioned such that when the LED board is placed into the slots, the LED's are centered in space in the window. Slightly behind the slots for the LED board is a circular crevice which is a pocket to contain the Melexis infrared temperature sensor. The temperature sensor is positioned so that it measures at an area in the middle of the tape being exposed to illumination by the wand. There are also four screw bosses used to attach the two pieces together. In the front of the wand is a window slot which is where the sodium chloride window is placed. There are additional features such as the curvature of the front panel and small fillets around the sides of the device. The reasons for these features was to not have sharp edges or corners which could potentially cause discomfort to a user/patient.

After printing out the parts, we noticed that we underestimated the space requirement for cables so we moved the bosses to corners of the part. We also reduced the width of the device because we noticed that it felt wide and difficult to grab. There were also holes added in the back of the wand for a USB slot in the Arduino, as well as a power cord for the system. Other changes

included air holes on the side of the wand to help with the fans located on the back of the LED board. The second-generation wand design is shown below in Figure 5.19 - Figure 5.22.

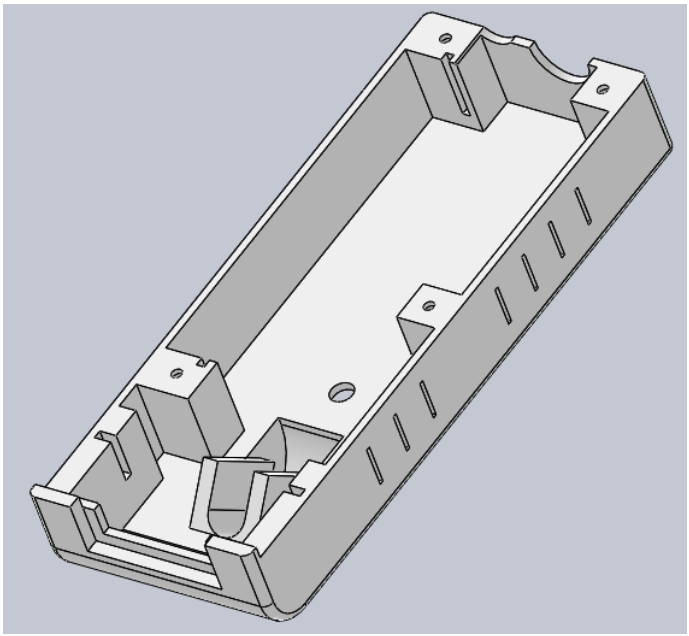

Figure 5.19. UnTape Wand 2nd Gen Top Section

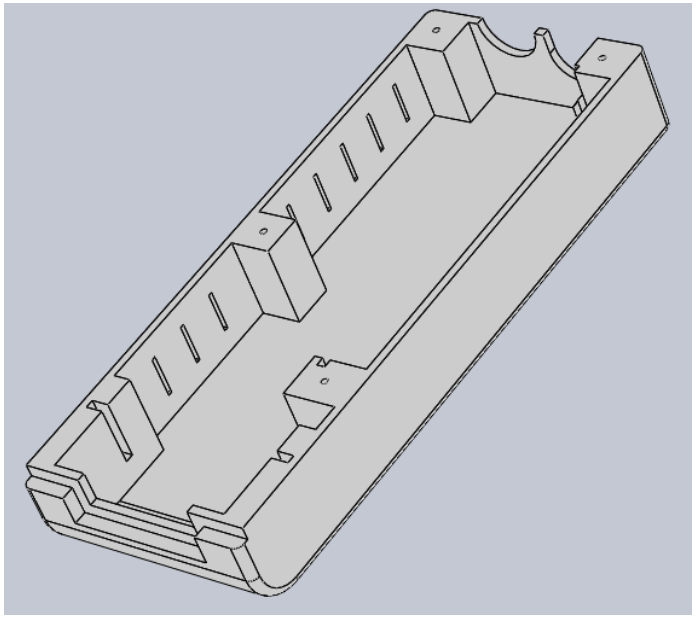

Figure 5.20. UnTape Wand 2nd Gen Bottom Section

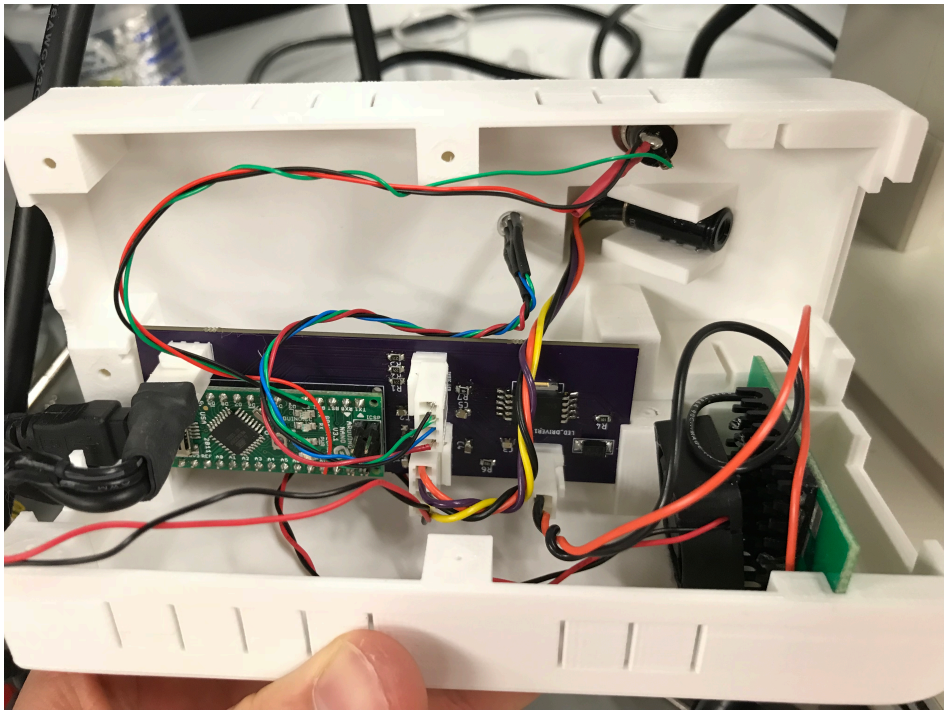

Figure 5.21. UnTape Wand 2nd Gen Internal Assembly

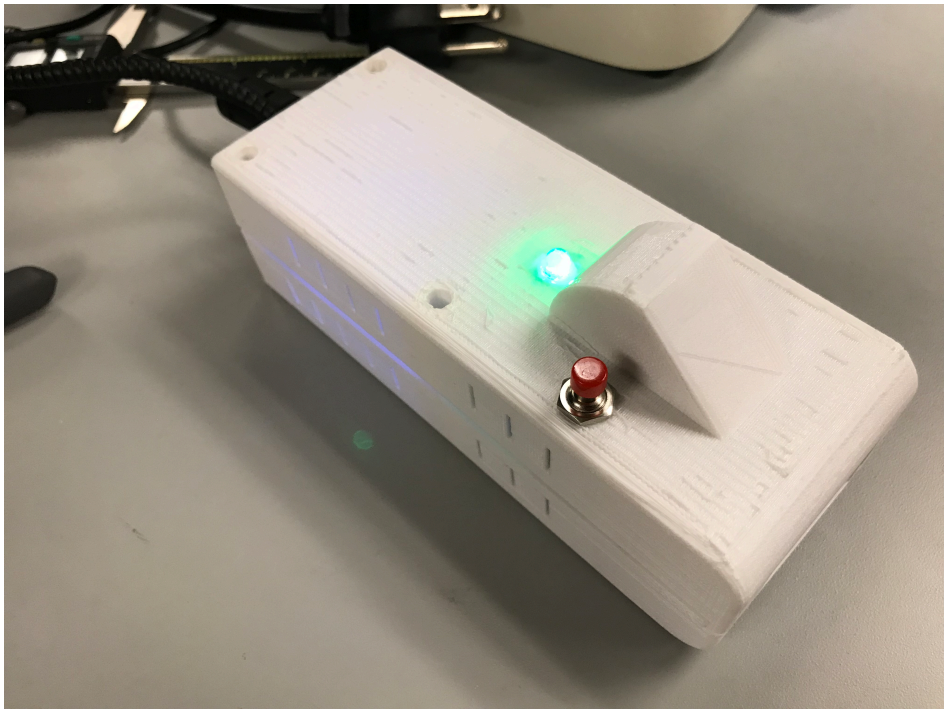

Figure 5.22. UnTape Wand 2nd Gen Exterior View

The second-generation wand fit all of the pieces well, however the fan behind the LED board was not stationary and had degrees of freedom. Additionally, we needed to redesign the LED driver on the Arduino/LED driver board due to incorrect resistor values, and upon doing so needed to also add heat sinking to the back of the driver due to the amount of heat being dissipated. The third-generation wand design is the similar to the second-generation, however has structure to constrain the fans, and an added bump on the side of the wand for the heat sink & fan required in the LED driver heat dissipation. The third-generation wand design is shown below in Figure 5.23 - Figure 5.26.

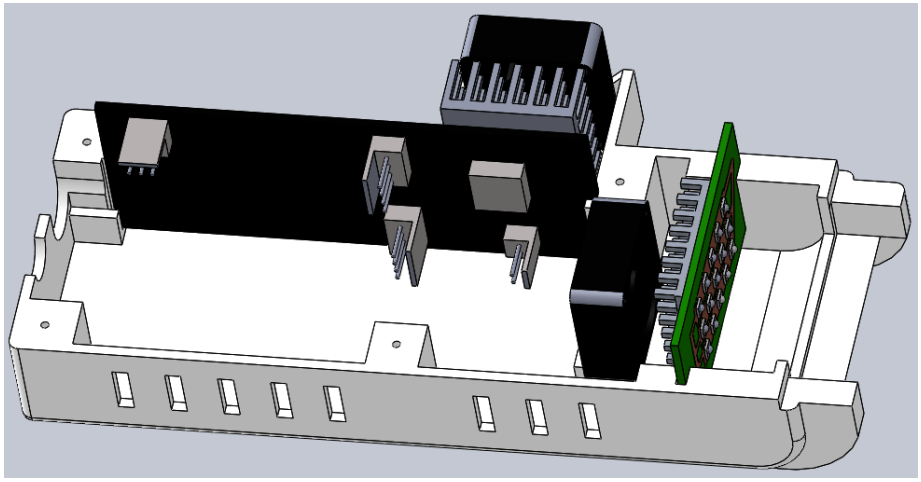

Figure 5.23. UnTape Wand 3rd Gen Internal View

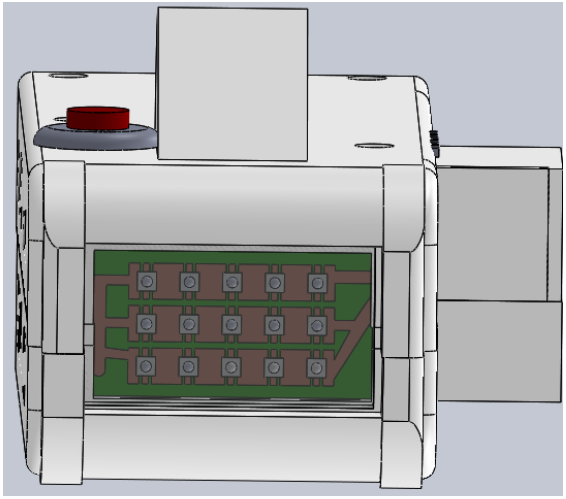

Figure 5.24. UnTape Wand 3rd Gen Front View

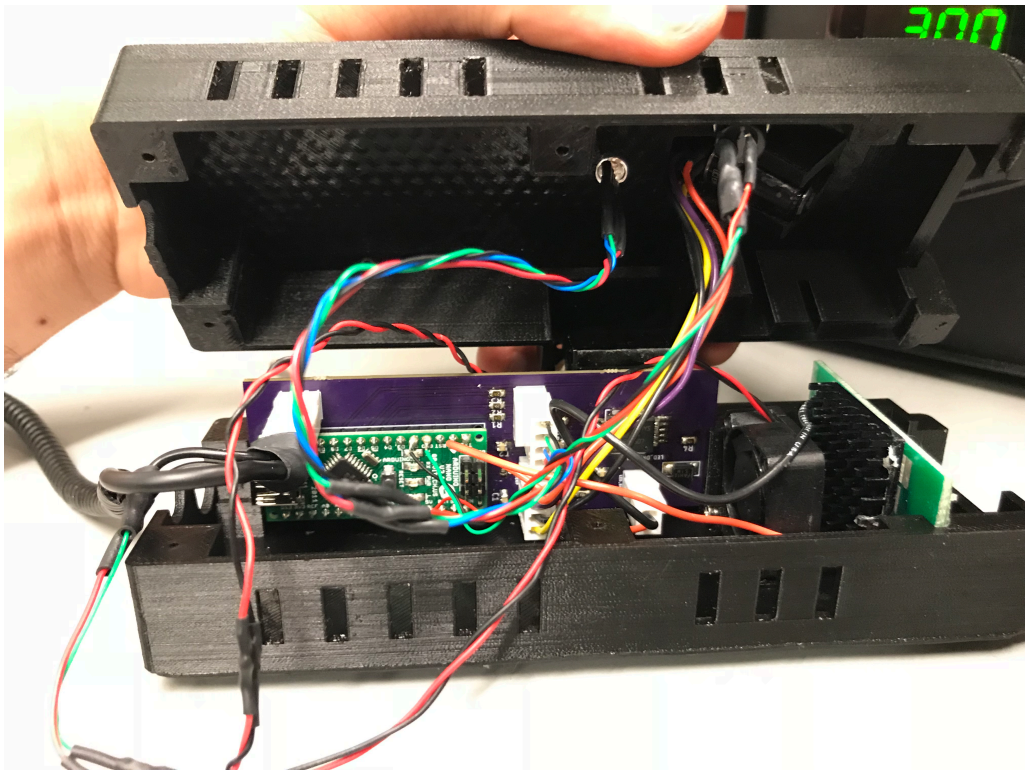

Figure 5.25. UnTape Wand 3rd Gen Internal Assembly

Figure 5.26. UnTape Wand 3rd Gen Exterior View

5.5 Future Design

In the future it is desired to have an UnTape wand that is much smaller and similar to a pocket flashlight which nurses can place in their pocket and recharge. Understanding this, there are many simplifications that need to occur with the current prototypes of the wand, not only with the size and shape of the wand design, but also with the power supply required by the current design. One of the major design flaws of the current design is the conservation of space and placement of the non-contact infrared temperature sensor. In order to optimize space usage, the sensor will be required to be in the middle of the case instead of on the outside. Additionally, there will need to be less LEDs in the design to save space.

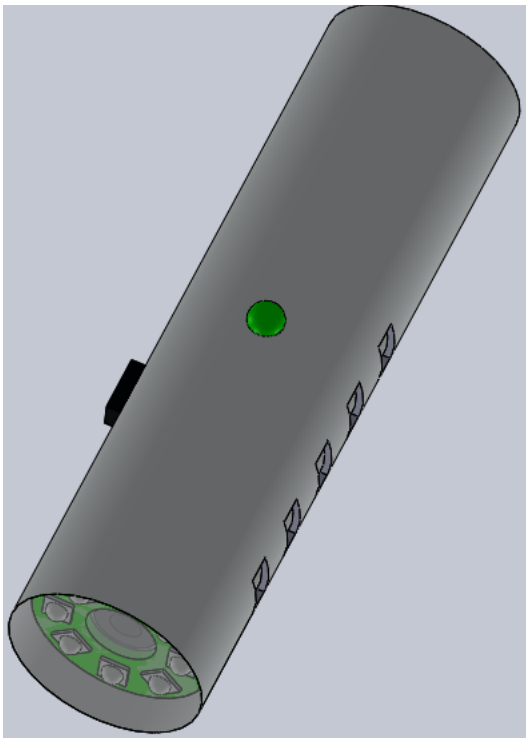

Figure 5.27. Possible Future UnTape Prototype

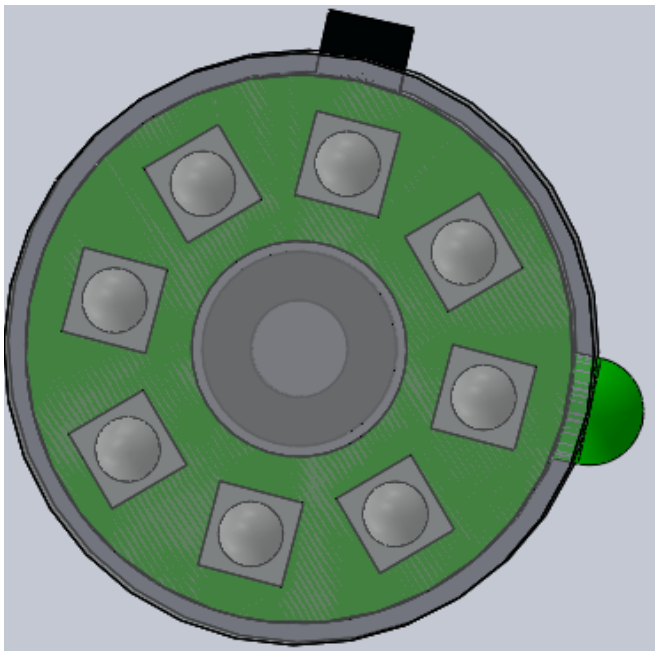

Figure 5.28. Possible Future UnTape Prototype Front View

The reason why such a large power supply was required in the design was because there is a lot of power required to get a piece of UnTape to 55C° in a short amount of time. Ideally, the temperature at which the UnTape loses a majority of its adhesion is in the 44C° range, which will require a lot less power internally. In order to spec a future design, we first needed to determine the amount of power required to get UnTape to 44C°. Since we already had a 2D Comsol skin model, we tested different values of power to find requirements for 5 second and 10 second rise times. With a 4000mW input we receive a 5 second rise time, and with a 3000mW input, a 10 second rise time. The results are shown below in Figure 5.27 & Figure 5.28.

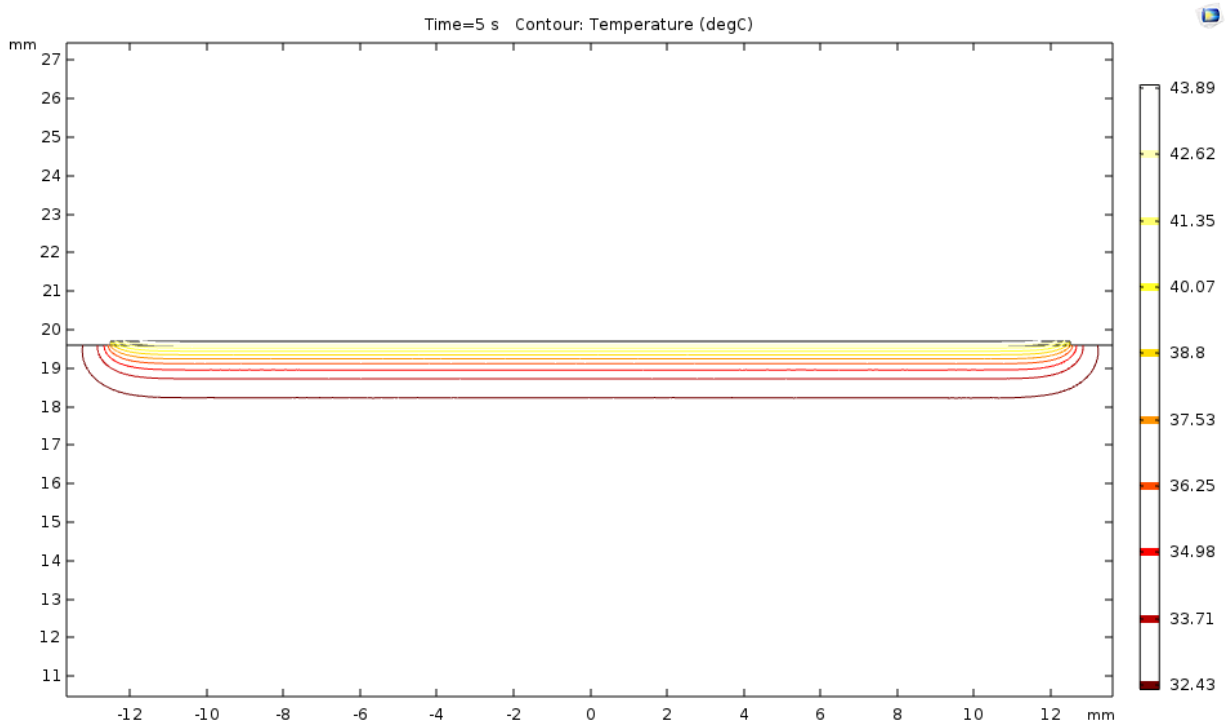

Figure 5.29. 2D Comsol Model on Skin with 4000mW Input

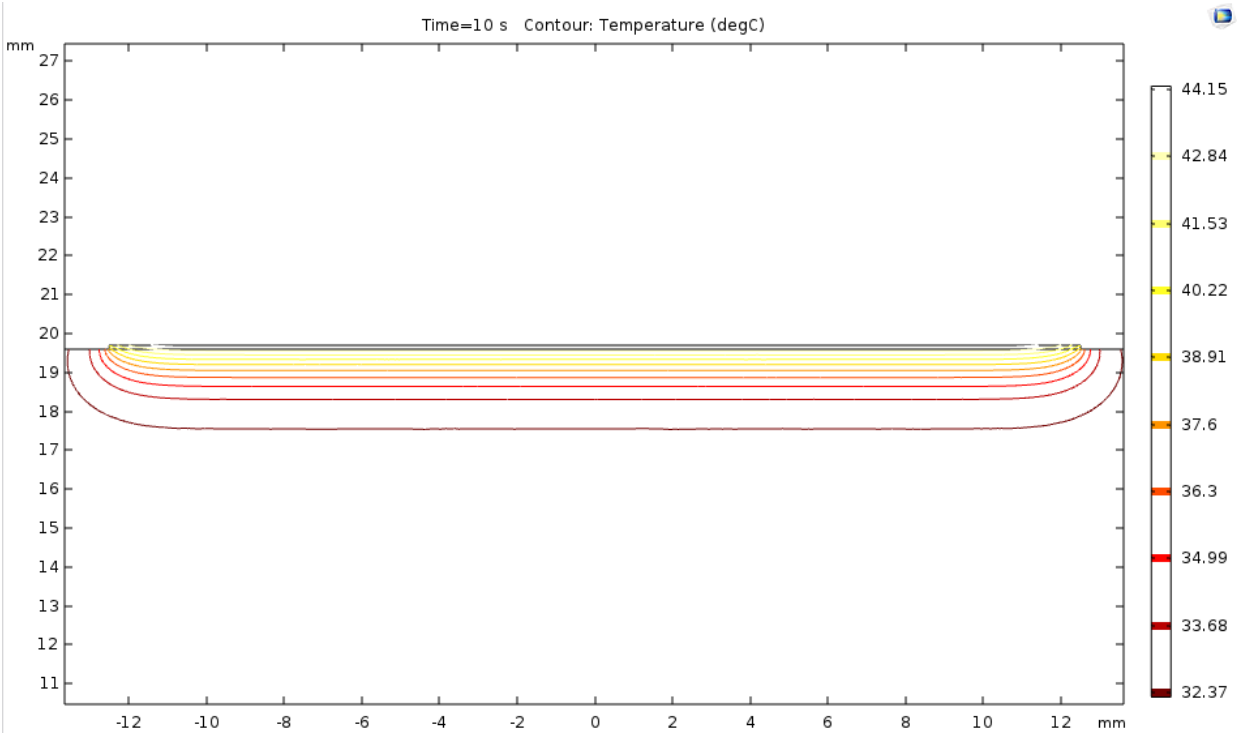

Figure 5.30. 2D Comsol Model on Skin with 3000mW Input

With this data populated, the next step is to determine the amount of power actually required to make that happen, since the UnTape does not absorb 100% of optical power. Table 5.1 - Table 5.3 show comparisons of optical power spec's and their relation to absorption by the Clearweld product.

Table 5.1. 50% Clearweld Absorption

	5s Rise Time	10s Rise Time
Required Power (mW)	4000	3000
Total Power Required (mW)	8000	6000
Power Req Per LED (8) (mW)	1000	750
LED Duty Cycle	.86	.65

Table 5.2. 70% Clearweld Absorption

	5s Rise Time	10s Rise Time
Required Power (mW)	4000	3000
Total Power Required (mW)	5714	4285
Power Req Per LED (8) (mW)	714	535
LED Duty Cycle	.62	.46

Table 5.3. 85% Clearweld Absorption

	5s Rise Time	10s Rise Time
Required Power (mW)	4000	3000
Total Power Required (mW)	4705	3529
Power Req Per LED (8) (mW)	588	441
LED Duty Cycle	.51	.38

From the tables above, it is clear that in order to minimize the power requirement in the device, we will need to increase the effectiveness of the Clearweld product absorption on the UnTape. Better absorption will require less power which will cut costs and improve battery life. In terms of battery life, ideally this product will be rechargeable, similar to the induction charging method used in Phillips Sonicare toothbrushes.

Chapter 6. CONCLUSION

From our results, we were able to show a proof of concept that the UnTape before release is similar in adhesion strength to the strongest commonly used medical tape, Durapore. After release, the UnTape is similar in weakness as the weakest commonly used medical tape, Kind. We were able to show that we can manipulate and control the temperature of the UnTape to reach a desired set point temperature extremely quickly, and that the thermal properties of skin dissipate heat extremely quickly below the surface of the skin. With the UnTape device, we can lower the incidence of medical adhesive related skin injuries with the ability to control the adhesion strength. This will not only add safety for more reliable and stronger adhesion, but also effectively save time and effort for nurses and administrators.

Future considerations for the optical wand design and fabrication mostly deal with the optimization of space and minimization of power usage. Ideally this product would be in the same size as a flashlight carried by nurses, meaning that it's not an added device that needs to be carried around but is integrated into perhaps an existing device, just adding functionality. It is also completely plausible to venture into different types of wound closure medical tape fields that require higher levels of adhesion because our product can still be easily removed.

There are a couple limitations of the current UnTape that we are working with. The first limitation is that the current UnTape has a high adhesion switch temperature at 55 C°. Ideally this temperature is at least 10 degrees less because 44 C° is considered to be the threshold at which skin begins to feel discomfort [21]. We will be attempting to synthesize a new UnTape at the University of Washington Chemistry department with a lower switch temperature, as well as embedded with the Clearweld product.

BIBLIOGRAPHY

[1] Food and Drug Administration Department of Health and Human Services, "Code of Federal Regulations Title 21, Section 880.5240: Medical adhesive tape and adhesive bandage." 07-Nov-2016.

[2] A.-M. Taroc, "Staying out of sticky situations: How to choose the right tape for your patient.," *Wound Care Advisor*, vol. 4, no. 6, pp. 21–26, Dec. 2015.

[3] 3M, "Introducing 3M Kind Removal Silicone Tape." 2011.

[4] 3M, "3M™ Kind Removal Silicone Tape: Set the Blue Tape Standard." 3M, 2012.

[5] L. McNichol, C. Lund, T. Rosen, and M. Gray, "Medical Adhesives and Patient Safety: State of the Science," *Journal of Wound, Ostomy and Continence Nursing*, vol. 40, no. 4, pp. 365–380, 2013.

[6] C. Lund, "Medical Adhesives in the NICU," *Newborn and Infant Nursing Reviews*, vol. 14, no. 4, pp. 160–165, Dec. 2014.

[7] S. Hunter, J. Anderson, D. Hanson, P. Thompson, D. Langemo, and M. G. Klug, "Clinical trial of a prevention and treatment protocol for skin breakdown in two nursing homes," *J Wound Ostomy Continence Nurs*, vol. 30, no. 5, pp. 250–258, Sep. 2003.

[8] M. J. Roberts, "Preventing and managing skin tears: a review," *Journal of Wound Ostomy & Continence Nursing*, vol. 34, no. 3, pp. 256–259, 2007.

[9] C. Konya *et al*., "Skin injuries caused by medical adhesive tape in older people and associated factors," *Journal of Clinical Nursing*, vol. 19, no. 9–10, pp. 1236–1242, May 2010.

[10] G. L. Grove, C. R. Zerweck, T. P. Houser, G. E. Smith, and N. I. Koski, "A Randomized and Controlled Comparison of Gentleness of 2 Medical Adhesive Tapes in Healthy Human Subjects:," *Journal of Wound, Ostomy and Continence Nursing*, vol. 40, no. 1, pp. 51–59, 2013.

[11] R. F. Holmes, M. W. Davidson, B. J. Thompson, and T. J. Kelechi, "Skin tears: care and management of the older adult at home," *Home Healthcare Now*, vol. 31, no. 2, pp. 90–101, 2013.

[12] S. Manriquez, B. Loperfido, and G. Smith, "Evaluation of a New Silicone Adhesive Tape among Clinicians Caring for Patients with Fragile or At-Risk Skin," *Advances in skin & wound care*, vol. 27, no. 4, pp. 163–170, 2014.

[13] M. K. Farris, M. Petty, J. Hamilton, S.-A. Walters, and M. A. Flynn, "Medical Adhesive-Related Skin Injury Prevalence Among Adult Acute Care Patients: A Single-Center Observational Study," *Journal of Wound, Ostomy and Continence Nursing*, vol. 42, no. 6, pp. 589–598, 2015.

[14] Y. Al-Nuaimi, M. J. Sherratt, and C. E. M. Griffiths, "Skin health in older age," *Maturitas*, vol. 79, no. 3, pp. 256–264, Nov. 2014.

[15] M. O. Visscher, R. Adam, S. Brink, and M. Odio, "Newborn infant skin: Physiology, development, and care," *Clinics in Dermatology*, vol. 33, no. 3, pp. 271–280, May 2015.

[16] M. Visscher and V. Narendran, "Neonatal Infant Skin: Development, Structure and Function," *Newborn and Infant Nursing Reviews*, vol. 14, no. 4, pp. 135–141, Dec. 2014.

[17] S. B. Hoath and H. I. Maibach, *Neonatal skin: structure and function*. New York: Marcel Dekker, Inc., 2003.

[18] C. H. Lund and J. A. Tucker, "Adhesion and newborn skin," in *Neonatal skin: structure and function*, S. B. Hoath and H. I. Maibach, Eds. New York: Marcel Dekker, Inc., 2003, pp. 299–324.

[19] K. M. McLane, K. Bookout, S. McCord, J. McCain, and L. S. Jefferson, "The 2003 national pediatric pressure ulcer and skin breakdown prevalence survey: a multisite study," *Journal of Wound Ostomy & Continence Nursing*, vol. 31, no. 4, pp. 168–178, 2004.

[20] C. Noonan, S. Quigley, and M. A. Q. Curley, "Skin Integrity in Hospitalized Infants and Children," *Journal of Pediatric Nursing*, vol. 21, no. 6, pp. 445–453, Dec. 2006.

[21] D. Yarnitsky, E. Sprecher, R. Zaslansky, J. A. Hemli, "Heat pain thresholds: normative data and repeatablility," *Pain,* vol. 60, no. 3, pp. 329-332, 1995.

[22] NCBI (2012). *Quick-Release Medical Tape* [Online]. Available FTP: https://www.ncbi.nlm.nih.gov Directory: /pmc/articles/PMC3503228/

[23] 3M Health Care Products (2015). Skin vs. Stainless Steel Adhesion Testing for Medical Design [Online]. Available FTP: http://multimedia.3m.com/ Directory /mws/media/876307O/skin-vs-stainless-steel-adhesion-testing.pdf

[24] Millington, P F. "Skin: Biological Structure and Function 9." *Skin: Biological Structure and Function 9*, edited by R Wilkinson, Cambridge University Press, 1983, pp. 127.

[25] Engineering ToolBox, (2003). *Thermal Conductivity of common Materials and Gases*. [Online] Available FTP: https://www.engineeringtoolbox.com/ Directory thermal-conductivity-d_429.html

[26] B. Laulicht, R. Langer, J.M. Karp "Quick-release medical tape," *Proceedings of the National Academy of Sciences,* vol 109, no. 46, pp 18803-18808, November 2012.

[27] 3M Health Care Products (2014). Medical Adhesive Related Skin Injuries (MARSI) [Online]. Available FTP: http://multimedia.3m.com/ Directory mws/media/1079841O/marsi-taping-techniques-1403-00577e-pdf.pdf

[28] 3M Health Care Products (2014). Medical Tapes [Online]. Available FTP: http://solutions.3m.com/ Directory wps/portal/3M/en_EU/Healthcare-Europe/EU-Home/Products/SkinWoundCare/MedicalTapes/

[29] ePlastics (2018). Plexiglass Sheets Infrared Transmitting [Online]. Available FTP: http://www.eplastics.com/ Directory Plexiglass_Acrylic_Sheet_Infrared_Transmitting

[30] Edmund Optics (2018). Sodium Chloride (NaCl) Windows [Online]. Available FTP: https://www.edmundoptics.com/ Directory optics/windows-diffusers/ultraviolet-uv-infrared-ir-windows/sodium-chloride-nacl-windows/

[31] Mouser Electronics (2015). Melexis Microelectric Integrated Systems: MLX90614 family [Online]. Available FTP: http://www.mouser.com/ Directory ds/2/734/MLX90614-Datasheet-Melexis-953298.pdf

[32] ThermoWorks, Inc (2018). Emissivity Table [Online]. Available FTP: https://www.thermoworks.com/ Directory emissivity_table

[33] Nitta Corporation (2018). Warm-Off Type [Online]. Available FTP: http://www.nitta.co.jp/ Directory en/?post_type=intelimer&p=8091

[34] IT'IS Foundation (2018). Heat Capacity [Online]. Available FTP: https://www.itis.ethz.ch/ Directory virtual-population/tissue-properties/database/heat-capacity/

[35] Multiple Sources. Densities of Different Body Matter [Online]. FTP: http://www.scrollseek.com/ Directory training/densitiesofdifferentbodymatter.html

[36] MatWeb: Material Property Data (2018). Overview of Materials for Acrylic, Cast [Online]. FTP: http://www.matweb.com/ Directory search/datasheet.aspx?bassnum=O1303&ckck=1 3

[37] Clearweld (2007). Clearweld 900 Series [Online]. FTP: http://www.clearweld.com/ Directory cms-assets/documents/Clearweld_900_Series_Coatings_Guide-web.pdf

[38] Mouser Electronics (2018). Luxeon IR Domed Line [Online]. FTP: https://www.mouser.com/ Directory datasheet/2/602/DS191-1138379.pdf